LA-UR-04-2260
FNAL-PUB-04-263-A
KRL-MAP-303

Cosmological Lepton Asymmetry, Primordial Nucleosynthesis and Sterile Neutrinos

Kevork Abazajian[1,2,3], Nicole F. Bell[2,3,4], George M. Fuller[3,5], Yvonne Y. Y. Wong[3]
[1] *Theoretical Division, MS B285, Los Alamos National Laboratory, Los Alamos NM 87545*
[2] *Theoretical Astrophysics, Fermi National Accelerator Laboratory, Batavia IL 60510*
[3] *Kavli Institute for Theoretical Physics, University of California, Santa Barbara, California 93106*
[4] *Kellogg Radiation Laboratory, California Institute of Technology, Pasadena, California 91125*
[5] *Department of Physics, University of California, San Diego, La Jolla, CA 92093-0319*
(Dated: October 7, 2004)

We study post weak decoupling coherent active-sterile and active-active matter-enhanced neutrino flavor conversion in the early universe. We find that under some circumstances sterile neutrino production via these processes can leave the active neutrinos with non-thermal energy spectra. In turn, these distorted energy spectra can affect primordial nucleosynthesis by altering the neutron-to-proton ratio. Inclusion of this effect changes the relationship between the cosmological lepton numbers and the primordial ^{4}He yield and reduces the range of lepton numbers that could reconcile the observationally-inferred primordial helium abundance with active-sterile vacuum neutrino mixing in the mass-squared difference range $0.2\,\mathrm{eV}^2 < \delta m^2 < 10\,\mathrm{eV}^2$. This δm^2 regime currently is being probed by accelerator-based experiments (mini-BooNE).

PACS numbers: 14.60.Pq; 14.60.St; 26.35.+c; 95.30.-k

I. INTRODUCTION

In this paper we study the cosmological lepton number-driven conversion of active neutrinos, ν_α (and/or $\bar{\nu}_\alpha$) with $\alpha = \mathrm{e}, \mu, \tau$, to a singlet, "sterile" neutrino species ν_s (or $\bar{\nu}_s$) in the post-weak decoupling environment of the early universe. We go on to assess the impact of this process on Big Bang Nucleosynthesis (BBN) and to examine critically the consequent prospects for reconciling the primordial helium abundance with neutrino mass-squared differences that lie in the range $0.2\,\mathrm{eV}^2 < \delta m^2_{\rm as} < 100\,\mathrm{eV}^2$ by means of a cosmological primordial lepton number. This neutrino mass-squared range is significant because it has been invoked to give a vacuum neutrino oscillation explanation for the LSND experiment's result [1] and it is covered by the on-going mini-BooNE experiment [2].

A positive signal in mini-BooNE, *i.e.*, confirming the interpretation of the LSND result in terms of vacuum neutrino mixing, sets up an immediate crisis in neutrino physics. Such a result, when combined with the already well established evidence for neutrino mixing at mass-squared differences associated with the atmospheric ($\delta m^2 \sim 3 \times 10^{-3}\,\mathrm{eV}^2$) and solar neutrino ($\delta m^2 \sim 7 \times 10^{-5}\,\mathrm{eV}^2$) anomalies, would suggest the existence of three independent neutrino mass-squared differences which would, in turn, require four neutrino species. Given the Z^0-width limit on the number of flavors of neutrinos with standard weak interactions (3), a fourth neutrino would have to be "sterile," with sub-weak interaction strength, *e.g.*, perhaps an SU(2) singlet. The only alternative to this line of reasoning and to this conclusion is the possibility of CPT violation [3]. However, there is no consistency of the neutrino oscillation data with a CPT-violating three-neutrino model at a 3-σ level [4].

Hand-in-hand with this particle physics dilemma, evidence for a singlet neutrino that mixes with active neutrinos in this mass-squared range also confronts cosmology with a curious and vexing problem. In the standard cosmological model with zero or near-zero net lepton numbers one would expect that matter-supressed neutrino oscillations in the channel $\nu_\alpha \rightleftharpoons \nu_s$ or in $\bar{\nu}_\alpha \rightleftharpoons \bar{\nu}_s$ (where $\alpha = e, \mu, \tau$) proceeding in the regime above weak interaction decoupling ($T > 3\,\mathrm{MeV}$), would efficiently populate seas of singlet neutrinos [5]. The significant additional energy density in these sterile neutrino seas would engender a faster expansion rate for the universe and a consequently higher temperature for Weak Freeze-Out (where the initial isospin of the universe, the neutron-to-proton ratio is set). A higher Weak Freeze-Out temperature would result in more neutrons and, hence, a higher yield of ^{4}He.

A higher predicted abundance of ^{4}He *arguably* may be in conflict (or close to being in conflict) with the observationally-inferred upper limit on the primordial helium abundance. Depending on the helium abundance inferred from compact blue galaxies, an increase in the predicted BBN ^{4}He yield may or may not be disfavored [5, 6]. However, the primordial helium abundance is notoriously difficult to extract from the observational data and recent studies point to a fair range for the observationally-inferred primordial mass helium fraction: 23% to 26% [7]. The upper limit of this range is provocatively close to the standard BBN ^{4}He mass fraction yield prediction, $24.85 \pm 0.05\%$, as computed with the deuterium-determined or CMB (Cosmic Microwave Background) anisotropy-determined baryon density.

Additionally, it has been suggested [8] that a fully populated sea of sterile neutrinos and antineutrinos with rest masses $\sim \sqrt{\delta m^2_{\rm as}}$ could be in conflict with neutrino mass bounds derived from CMB anisotropy limits and large scale structure considerations [9]. There is a recent analysis of constraints from measurements of galaxy bias stemming from galaxy-galaxy lensing and the inferred linear matter power spectrum derived from the Lyman alpha forest in the Sloan Digital Sky Survey (SDSS) [10]. This analysis specifically considers a so-called "3+1" neutrino mass hierarchy, *i.e.,* the scheme which is appropriate for constraining sterile neutrinos. The neutrino mass constraint so derived is somewhat less stringent than constraints in schemes with three neutrinos with degenerate masses. However, the central conclusions of Ref. [8] survive.

Should we someday be confronted with a positive indication of neutrino flavor mixing with mass-squared scale consistent with the range for $\delta m^2_{\rm as}$, we will have a problem that would call for modification either of our notions of basic neutrino physics or of the standard cosmological model. There have been a number of ways proposed to get out of these cosmological problems. Chief among these is the invocation of a significant net lepton number in the universe [11]. The idea is that the net lepton number gives active neutrinos larger effective masses in medium in the early universe, thereby driving them further off-resonance in the epoch prior to weak decoupling (*i.e.*, $T > 3\,{\rm MeV}$) and reducing their effective matter mixing angles with the singlet neutrino. In turn, smaller effective matter mixing angles would imply a suppressed production of singlet neutrinos and, hence, a reduced population of the singlet neutrino sea.

The lepton number residing in the sea of ν_α and $\bar{\nu}_\alpha$ neutrinos ($\alpha = e, \mu, \tau$) is defined in analogy to the baryon number $\eta \equiv (n_b - n_{\bar{b}})/n_\gamma \approx 6 \times 10^{-10}$,

$$L_{\nu_\alpha} = \frac{n_{\nu_\alpha} - n_{\bar{\nu}_\alpha}}{n_\gamma} \tag{1}$$

where $n_\gamma = \left(2\zeta(3)/\pi^2\right) T_\gamma^3$ is the proper photon number density at temperature T_γ, and where n_{ν_α} and $n_{\bar{\nu}_\alpha}$ are the number densities of ν_α and $\bar{\nu}_\alpha$ neutrinos, respectively, at this epoch.

We can insure that the effective matter mixing angles for the oscillation channel $\nu_\alpha \rightleftharpoons \nu_s$ (or $\bar{\nu}_\alpha \rightleftharpoons \bar{\nu}_s$) are sufficiently small to suppress singlet neutrino production if the Mikheyev-Smirnov-Wolfenstein (MSW) [12] resonance temperature is less than the weak decoupling temperature, $T_{\rm res} < T_{\rm dec}$. This implies that the lepton number associated with any of the active neutrino flavors should satisfy,

$$L > \frac{10^{-3}}{\epsilon} \left(\frac{2}{N_{\rm degen}}\right) \left(\frac{3\,{\rm MeV}}{T_{\rm dec}}\right)^4 \left(\frac{\delta m^2_{\rm as} \cos 2\theta}{1\,{\rm eV}^2}\right) \tag{2}$$

where θ is the vacuum mixing angle characteristic of $\nu_\alpha \rightleftharpoons \nu_s$ oscillations, $N_{\rm degen}$ is the number of neutrino species possessing this lepton number, and where $\epsilon \equiv E_\nu/T$. For neutrinos with typical energies in the early universe (*i.e.*, $\epsilon \sim 1$), suppression of singlet neutrino production would require lepton numbers ranging from $L > 10^{-4}$ for $\delta m^2_{as} = 0.2\,{\rm eV}^2$ to $L > 5 \times 10^{-3}$ for $\delta m^2_{as} = 10\,{\rm eV}^2$. Current limits on lepton numbers are $|L_{\nu_\alpha}| < 0.1$ [13] (and possibly even weaker by a factor of two or so if allowance is made for another source of extra energy density in the early universe [14]). Therefore, this avenue for escape from the sterile neutrino conundrum appears to be allowed, albeit at the cost of a huge disparity between the lepton and baryon numbers.

However, this argument overlooks an important point. Though the large lepton number supresses the effective matter mixing angle for $\nu_\alpha \rightleftharpoons \nu_s$ during the epoch of the early universe where active neutrinos are thermally coupled ($T > T_{\rm dec}$), it can cause coherent matter-enhancement of this channel at lower temperatures where the active neutrinos rarely scatter and are effectively decoupled. Resonant MSW transformation of active neutrinos to singlets in the channel $\nu_\alpha \rightleftharpoons \nu_s$ is, however, self limiting. This is because as the universe expands and the resonance sweeps from low toward higher neutrino energy, the conversion of ν_α's decreases the lepton number which, in turn, causes the resonance sweep rate to increase, eventually causing neutrinos to evolve non-adiabatically through resonance and so causing flavor transformation to cease.

At issue then is how many active neutrinos can be converted to sterile neutrinos prior to Weak Freeze-Out, where the neutron-to-proton ratio is set. If there is a significant conversion, the resultant non-thermal active neutrino energy spectra can cause an increase or decrease (if $\bar{\nu}_\alpha \rightleftharpoons \bar{\nu}_s$ is enhanced) in the ^{4}He yield and call into question the viability of invoking a large net lepton number to reconcile neutrino physics and BBN. Other but related aspects of transformation-induced nonthermal neutrino spectra effects on primordial nucleosynthesis have been studied in Ref.s [15, 16]. In any case, non-thermal energy distribution functions for ν_e and/or $\bar{\nu}_e$ change the relationship between the BBN ^{4}He yield and the neutrino chemical potentials.

In section II we discuss the physics of active-sterile neutrino flavor transformation in the early universe and the physics that determines how the MSW resonance sweeps through the neutrino energy distribution functions as the universe expands. The adiabaticity of neutrino flavor evolution in general is also discussed in this section, as is simultaneous active-active and active-sterile neutrino flavor conversion, and "synchronization." Possible multi-neutrino mass level crossing scenarios in the early universe are discussed in this section. Sterile neutrino contributions to closure, constraints on this from large scale structure and Cosmic Microwave Background radiation considerations, as well as other sterile neutrino sea population constraints are examined in section III. In section IV we describe how distorted ν_e and/or $\bar{\nu}_e$ distribution functions impact the rates of the lepton capture reactions that determine the neutron-to-proton ratio and the ^{4}He

yield in BBN. This is then applied in various initial lepton number and neutrino conversion scenarios. Finally, in section V we give conclusions and speculations regarding the neutrino mass and cosmological lepton number insights that would follow in the wake of an experimental signature for a large neutrino mass-squared difference of order the range given for δm^2_{as}. Appendix A provides an exposition of the lepton capture rates on free nucleons when, as appropriate, ν_e or $\bar{\nu}_e$ energy distribution functions are zero up to some energy, and thermal/Fermi-Dirac at higher energies.

II. COHERENT NEUTRINO FLAVOR TRANSFORMATION IN THE EARLY UNIVERSE

A. Active-Sterile Conversion

Coherent conversion of active neutrino species into singlets in the early universe can occur through the usual MSW process, albeit in an exotic setting. In words, this process is extremely simple: (1) an active neutrino (mostly the light mass state in vacuum) forward scatters on particles in the plasma and, if there is a net lepton and/or baryon number, will acquire a positive effective mass; (2) when this effective mass is close to the mass associated with the singlet (mostly the heavy mass state), transformation of flavors can occur. The efficiency of conversion at such a mass level crossing (or MSW resonance) depends on the ratio of the resonance width (in time or space) to the neutrino oscillation length. Efficient, adiabatic conversion takes place only when this ratio is large.

The forward charged and neutral current exchange Hamiltonians for the neutrinos in the early universe are as follows:

$$H\left(\nu_s\right) = 0 \tag{3}$$

$$H\left(\nu_e\right) = \sqrt{2}G_{\rm F}\left(n_e - \frac{1}{2}n_n\right) + \sqrt{2}G_{\rm F}\left(2\left(n_{\nu_e} - n_{\bar{\nu}_e}\right) + \left(n_{\nu_\mu} - n_{\bar{\nu}_m u}\right) + \left(n_{\nu_\tau} - n_{\bar{\nu}_\tau}\right)\right) \tag{4}$$

$$H\left(\nu_\mu\right) = \sqrt{2}G_{\rm F}\left(-\frac{1}{2}n_n\right) + \sqrt{2}G_{\rm F}\left(\left(n_{\nu_e} - n_{\bar{\nu}_e}\right) + 2\left(n_{\nu_\mu} - n_{\bar{\nu}_m u}\right) + \left(n_{\nu_\tau} - n_{\bar{\nu}_\tau}\right)\right) \tag{5}$$

$$H\left(\nu_\tau\right) = \sqrt{2}G_{\rm F}\left(-\frac{1}{2}n_n\right) + \sqrt{2}G_{\rm F}\left(\left(n_{\nu_e} - n_{\bar{\nu}_e}\right) + \left(n_{\nu_\mu} - n_{\bar{\nu}_m u}\right) + 2\left(n_{\nu_\tau} - n_{\bar{\nu}_\tau}\right)\right). \tag{6}$$

Here $n_e = n_{e^-} - n_{e^+}$ is the net number density of electrons, $n_n = n_b - n_p$ is the number density of neutrons, and n_b and n_p are the net number densities of baryons and protons, respectively. Charge neutrality implies that the number density of protons is $n_p = n_e = n_b Y_e$. The net number of electrons per baryon is Y_e. The baryon number density is $n_b \approx \eta n_\gamma$, where the baryon-to-photon ratio η is as defined above.

Weak Decoupling occurs when neutrino scattering becomes so slow that it can no longer facilitate efficient energy exchange between the neutrino gas and the plasma. For the low lepton numbers considered here, Weak Decoupling occurs at temperature $T \sim 3\,\mathrm{MeV}$.

Weak Freeze-Out occurs when the rates of the reactions that govern the ratio of neutrons-to-protons ($n/p = 1/Y_e - 1$) fall below the expansion rate of the universe. This is roughly at $T \approx 0.7\,\mathrm{MeV}$ for standard cosmological parameters. Below this temperature Y_e is only slowly decreasing and this decrease is dominated by free neutron decay.

Note that in the regime between Weak Decoupling and Weak Freeze-Out, we have $Y_e \approx 0.5$. Therefore, throughout this epoch we will have nearly equal numbers of neutrons and protons. During this time we can then approximate $n_e - \frac{1}{2}n_n = n_b(\frac{3}{2}Y_e - \frac{1}{2}) \approx n_\gamma\eta/4$, and $-\frac{1}{2}n_n = n_b(Y_e/2 - \frac{1}{2}) \approx -n_\gamma\eta/4$.

We can denote the weak potentials from neutrino-electron charged current forward exchange scattering and neutrino-neutrino neutral current forward exchange scattering as A and B, respectively, with their sum being

$$A + B \approx \frac{2\sqrt{2}\zeta(3)G_{\rm F}T^3}{\pi^2}\left(\mathcal{L} \pm \frac{\eta}{4}\right), \tag{7}$$

where $G_{\rm F}$ is the Fermi constant, the Riemann Zeta function of argument 3 is $\zeta\left(3\right) \approx 1.20206$, and we take the plus sign for transformation of ν_e, and the minus sign for conversion of ν_μ and/or ν_τ. (Here the plus sign is taken when we intend $A + B = H(\nu_e)$ and the minus sign is taken when $A + B = H(\nu_{\mu,\tau})$.) A measure of the lepton number which enters into the potential for the $\nu_\alpha \rightleftharpoons \nu_s$

$(\alpha = e, \mu, \tau)$ conversion channel is

$$\mathcal{L} \equiv 2L_{\nu_\alpha} + \sum_{\beta \neq \alpha} L_{\nu_\beta}. \tag{8}$$

We will refer to this quantity as the "potential lepton number." In general this may be different for different channels $\nu_\alpha \rightleftharpoons \nu_s$, even for a given set of lepton numbers associated with each flavor.

Finally, since the early universe is at relatively high entropy per baryon, the overall weak potential has a contribution from neutrino neutral current forward scattering on a thermal lepton background. This thermal potential is

$$C \approx -r_\alpha G_{\rm F}^2 \epsilon T^5, \tag{9}$$

where the neutrino energy divided by the temperature is $\epsilon \equiv E_\nu/T$. For the conversion channel $\nu_e \rightleftharpoons \nu_s$, we employ $r_e^0 \approx 79.34$, while for the channel $\nu_{\mu,\tau} \rightleftharpoons \nu_s$, we use $r_{\mu,\tau}^0 \approx 22.22$. If the neutrinos have strictly thermal energy distribution functions, then

$$r_\alpha \approx r_\alpha^0 \left[\frac{F_2\left(\eta_{\nu_\alpha}\right)}{F_2\left(0\right)} + \frac{F_2\left(\eta_{\bar{\nu}_\alpha}\right)}{F_2\left(0\right)} \right], \tag{10}$$

where the neutrino and antineutrino degeneracy parameters are η_{ν_α} and $\eta_{\bar{\nu}_\alpha}$, respectively, and the Fermi integrals of order 2 are defined below. For the small lepton numbers considered in this paper, we can almost always use $r_e \approx r_e^0$ and $r_{\mu,\tau} \approx r_{\mu,\tau}^0$.

The total weak forward scattering potential is

$$V \approx A + B + C. \tag{11}$$

For the transformation channel $\nu_\alpha \rightleftharpoons \nu_s$, the neutrino mass level crossing (MSW resonance) condition for a neutrino with scaled energy ϵ is

$$\frac{\delta m^2 \cos 2\theta}{2\epsilon T} \approx V, \tag{12}$$

where δm^2 is the difference of the squares of the appropriate neutrino mass eigenvalues and θ is the relevant *effective* two-by-two vacuum mixing angle. Neglecting the light mass eigenvalue, the effective mass-squared acquired by an electron neutrino from forward scattering on weak charge-carrying targets in the early universe is

$$m_{\rm eff}^2 \approx 2\epsilon V \approx \left(8.03 \times 10^{-12}\,{\rm MeV}^2\right) \epsilon(\mathcal{L} \pm \eta/4) \left(\frac{T}{\rm MeV}\right)^4 - \left(2.16 \times 10^{-20}\,{\rm MeV}^2\right) \epsilon^2 \left(\frac{T}{\rm MeV}\right)^6. \tag{13}$$

It is clear that we can negelect the second term (the thermal term C) in Eq. (11) in the regime between Weak Decoupling and Weak Freeze-Out, where $3\,{\rm MeV} > T > 0.7\,{\rm MeV}$.

At a given temperature, the scaled neutrino energy which is resonant is

$$\epsilon_{\rm res} = \frac{\delta m^2 \cos 2\theta}{2VT}. \tag{14}$$

If we neglect the thermal term, the rough dependence of resonant energy on temperature and lepton number is

$$\begin{aligned} \epsilon_{\rm res} &\approx \frac{\pi^2 \delta m^2 \cos 2\theta}{2^{5/2}\zeta\left(3\right) G_{\rm F} (\mathcal{L} \pm \eta/4) T^4} \\ &\approx 0.124 \left(\frac{\delta m^2 \cos 2\theta}{1\,{\rm eV}^2}\right) \frac{1}{\mathcal{L}} \left(\frac{\rm MeV}{T}\right)^4, \end{aligned} \tag{15}$$

where in the second approximation we neglect the neutrino-electron forward scattering contribution $(\pm\eta/4)$ relative to $\mathcal{L}$. It is clear from Eq. (15) that as the universe expands and the temperature drops, the resonance energy $\epsilon_{\rm res}$ will sweep from lower to higher values. In fact, as the resonance sweeps through the active neutrino distribution, converting $\nu_\alpha \to \nu_s$, $\mathcal{L}$ will decrease, further accelerating the resonance sweep rate.

Assuming homogeneity and isotropy, the number density of active neutrinos ν_α with thermal distribution function $f_{\nu_\alpha}\left(\epsilon\right)$ in the scaled energy range ϵ to $\epsilon + d\epsilon$ is

$$dn_{\nu_\alpha} = n_{\nu_\alpha} f_{\nu_\alpha}\left(\epsilon\right) d\epsilon, \tag{16}$$

where n_{ν_α} is the total number density (that is, integrated over all neutrino energies). In terms of the temperature T and degeneracy parameter $\eta_{\nu_\alpha} \equiv \mu_{\nu_\alpha}/T$, where μ_{ν_α} is the appropriate chemical potential, the thermal distribution function is

$$f_{\nu_\alpha}\left(\epsilon\right) = \frac{1}{F_2\left(\eta_{\nu_\alpha}\right)} \frac{\epsilon^2 d\epsilon}{e^{\epsilon - \eta_{\nu_\alpha}} + 1}. \tag{17}$$

We define relativistic Fermi integrals of order k in the usual fashion:

$$F_k\left(\eta\right) \equiv \int_0^\infty \frac{x^k dx}{e^{x-\eta} + 1}. \tag{18}$$

The total number density of thermally distributed active neutrinos ν_α with temperature T_ν and degeneracy parameter η_{ν_α} is

$$n_{\nu_\alpha} = \frac{T_\nu^3}{2\pi^2} F_2\left(\eta_{\nu_\alpha}\right). \tag{19}$$

Note that if the neutrino degeneracy parameter is $\eta_{\nu_\alpha} = 0$, then $F_2\left(0\right) = 3\zeta\left(3\right)/2$ and the number density of thermally distributed ν_α's is

$$n_{\nu_\alpha} = \frac{3}{8} n_\gamma \left(\frac{T_\nu}{T_\gamma}\right)^3, \tag{20}$$

where we allow for the neutrino temperature T_ν to differ from the photon/plasma temperature T_γ.

The relationship between the lepton number in α flavor neutrinos and the ν_α degeneracy parameter is

$$L_{\nu_\alpha} \approx \left(\frac{\pi^2}{12\zeta\left(3\right)}\right)\left(\frac{T_\nu}{T_\gamma}\right)^3 \left[\eta_{\nu_\alpha} + \eta_{\nu_\alpha}^3/\pi^2\right]. \tag{21}$$

This relation assumes that neutrinos ν_α and antineutrinos $\bar{\nu}_\alpha$ are (or were at one point) in thermal equilibrium so that $\eta_{\bar{\nu}_\alpha} = -\eta_{\nu_\alpha}$. In the limit where the lepton number is small, so that $\eta_{\nu_\alpha} \ll 1$, and the neutrino and photon temperatures are nearly the same, we can approximate Eq. (21) as $\eta_{\nu_\alpha} \approx 1.46 L_{\nu_\alpha}$. Neutrino degeracy parameter is a comoving invariant; whereas, lepton number is not in general since the photons can be heated relative to the neutrinos by, *e.g.*, $e^\pm$ annihilation.

Some employ an "effective number of neutrino flavors" N_ν as a measure of both energy density in relativistic particles and the extent to which the energy density in the neutrino gas differs from that of pure Fermi-Dirac, zero chemical potential neutrino distributions. For one degenerate neutrino species the change in the effective number of neutrinos over the zero lepton number case, $N_\nu = 3$, is

$$\Delta N_\nu \approx \frac{30}{7}\left(\frac{\eta_{\nu_\alpha}}{\pi}\right)^2 + \frac{15}{7}\left(\frac{\eta_{\nu_\alpha}}{\pi}\right)^4. \tag{22}$$

As the universe expands and ν_α neutrinos are converted to sterile species ν_s, the lepton number L_{ν_α} drops. As $\mathcal{L}$ approaches zero, the resonance sweep rate becomes so large that neutrinos will be propagating through MSW resonances non-adiabatically [18]. Efficient neutrino flavor conversion ceases at this point. If the conversion process results in a change in the number density of ν_α neutrinos, Δn_{ν_α}, such that the lepton number associated with this species changes by $\Delta L_{\nu_\alpha} = -\Delta n_{\nu_\alpha}/n_\gamma$, then the potential lepton number would change from its initial value, $\mathcal{L}^{\rm initial}$ to

$$\mathcal{L}^{\rm final} = \mathcal{L}^{\rm initial} + 2\Delta L_{\nu_\alpha}. \tag{23}$$

The adiabaticity condition ensures that flavor conversion ceases when $\mathcal{L}^{\rm final}$ approaches zero, or in other words, when $\Delta L_{\nu_\alpha} = -\mathcal{L}^{\rm initial}/2$. It is important to note that transformation of *any flavor* active neutrino to sterile flavor can drive down the overall potential lepton number, no matter which flavor or flavors of active neutrinos harbor the net lepton number.

If additionally we were to assume that the resonance smoothly swept through the ν_α energy distribution from zero to energy ϵ during this conversion process, we would have $\Delta n_{\nu_\alpha} = \int_0^\epsilon dn_{\nu_\alpha}$ and so the concomitant change in lepton number would be

$$\Delta L_{\nu_\alpha} \approx -\frac{3}{8}\left(\frac{T_\nu}{T_\gamma}\right)^3 \frac{1}{F_2\left(0\right)} \int_0^\epsilon \frac{x^2}{e^{x-\eta_{\nu_\alpha}}+1}. \tag{24}$$

In this idealized limit, the potential lepton number as a function of ϵ, the scaled energy of resonance assuming a smooth and continuous resonance sweep from zero energy, is

$$\mathcal{L}(\epsilon) \approx \mathcal{L}^{\rm initial} - \frac{3}{4}\frac{1}{F_2\left(0\right)} \int_0^\epsilon \frac{x^2}{e^{x-\eta_{\nu_\alpha}}+1}. \tag{25}$$

In this last relation we have set the photon/plasma and neutrino temperatures to be the same. This is a good approximation in the epoch between Weak Decoupling and Weak Freeze-Out where we are interested in active-sterile neutrino conversion. This is because during this epoch there has been little annihilation of $e^\pm$ pairs and, consequently, little heating of the photons/plasma relative to the decoupled neutrinos.

Employing the approximation of a smooth and continuous sweep of scaled resonance energy from zero to ϵ, we can re-write the resonance condition, Eq. (15), as

$$\epsilon\mathcal{L}(\epsilon) \approx \frac{\pi^2 \delta m^2 \cos 2\theta}{2^{5/2}\zeta\left(3\right) G_{\rm F} T^4}, \tag{26}$$

where we have neglected the baryon number.

Eq. (26) reveals a problem: the resonance cannot sweep continuously and smoothly to the point where $\mathcal{L}(\epsilon) \to 0$. This is because $\epsilon\mathcal{L}(\epsilon)$ is a peaked function. The maximum of this function occurs for a value $\epsilon_{\rm max}$ satisfying the integral equation

$$\epsilon_{\rm max}^3 \approx 2\zeta\left(3\right)\left(e^{\epsilon_{\rm max}-\eta_{\nu_\alpha}}+1\right)\mathcal{L}(\epsilon_{\rm max}). \tag{27}$$

It is clear, however, that as the universe expands, the right hand side of Eq. (26) will increase monotonically. Although the resonance sweep can begin smoothly and continuously, there will come a point where it is no longer possible to find a solution to Eq. (26). This will occur when the resonance energy reaches $\epsilon_{\rm max}$.

What happens beyond this point? If we relax the demand that the resonance sweep be continuous, then it is possible in principle to find a solution to Eq. (26) as the temperature drops beyond the point where $\epsilon = \epsilon_{\rm max}$, though this would require a re-interpretation of $\mathcal{L}(\epsilon)$ in obvious fashion. For example, the resonance energy could skip to some value $\epsilon > \epsilon_{\rm max}$, possibly toward the higher energy portions of the neutrino distribution function. There the occupation number would be small and so the decrement in $\mathcal{L}(\epsilon)$ would be similarly small. It is even possible that beyond $\epsilon_{\rm max}$ the resonance sweeps stochastically through relatively small intervals of the active neutrino distribution function.

In any case, active-to-sterile neutrino conversion $\nu_\alpha \to \nu_s$ will have to cease when $\mathcal{L}$ approaches zero. At this

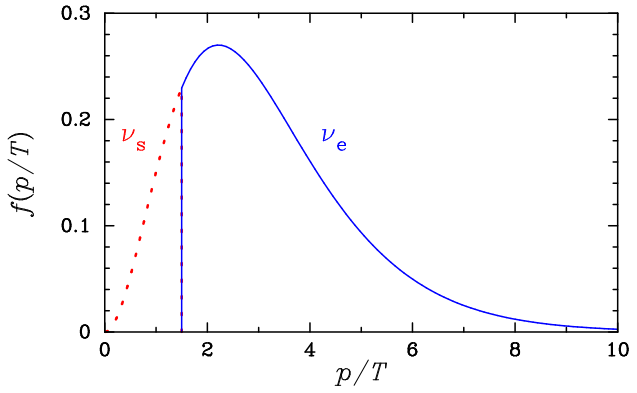

FIG. 1: The nonthermal scaled energy (p/T) distributions for ν_s (dotted) and ν_e (solid) resulting from smooth, adiabatic resonance sweep.

point we will be left with grossly non-thermal, non-Fermi-Dirac ν_α and ν_s distributions. Since this process occurs after Weak Decoupling, active neutrino inelastic scattering processes on electrons, nucleons, and other neutrinos have rates which are slow compared to the expansion rate of the universe. This means that these processes will be unable to redistribute the active neutrino occupation numbers and so they cannot morph the ν_α distribution into a thermal distribution. This has consequences for the lepton capture rates on nucleons as we will discuss below in section IV.

In the either the smooth and continuous resonance sweep limit or the stochastic resonance sweep limit both the active neutrino and resulting sterile neutrino distribution functions will be non-thermal in character. For the special case of a smooth and continuous and *adiabatic* resonance sweep up to a scaled energy limit, and an assumed non-adiabatic evolution thereafter for higher energy neutrinos, the resulting active and sterile neutrino distribution functions would be as shown in Fig. (1).

This energy distribution function is zero for all values of scaled neutrino energy $0 \leq E_\nu/T \leq \epsilon$, and has a normal Fermi-Dirac thermal distribution character for all neutrino energies $E_\nu/T > \epsilon$. The corresponding sterile neutrino energy spectrum would be the "mirror image" of this: a thermal Fermi-Dirac spectrum for $0 \leq E_\nu/T \leq \epsilon$, and zero occupation for $E_\nu/T > \epsilon$.

It is useful to consider the solution for the cut-off energy ϵ and the peak energy $\epsilon_{\rm max}$ in the smooth and continuous resonance sweep case. In this limit, the first of these quantities is the solution of

$$\mathcal{L}^{\rm initial} = \frac{3}{4}\frac{1}{F_2\left(0\right)}\int_0^\epsilon \frac{x^2}{e^{x-\eta_{\nu_\alpha}}+1}, \qquad (28)$$

or $\mathcal{L}\left(\epsilon\right) = 0$. The second of these quantities is the solution of Eq. (27). Both of these solutions are shown as functions of initial $\mathcal{L}$ in Fig. (2). In this figure it is assumed that the active neutrinos are fully "equilibrated" initially (before any flavor transformation) with $L_{\nu_e} = L_{\nu_\mu} = L_{\nu_\tau}$.

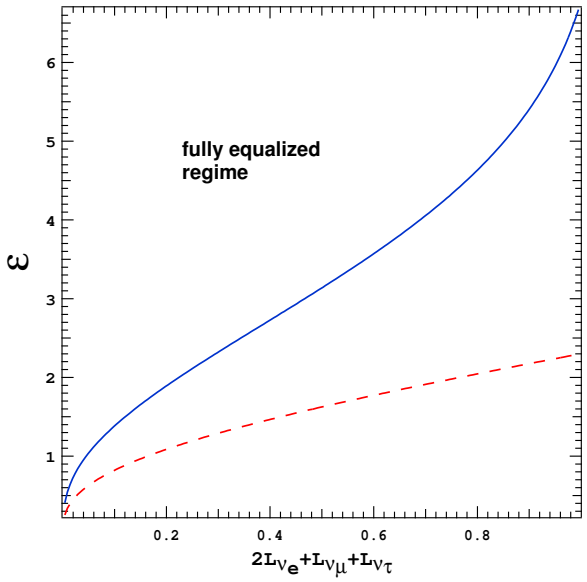

FIG. 2: The values of ϵ (solid line) and $\epsilon_{\rm max}$ (dashed line) are shown as functions of total initial potential lepton number in the limit of a smooth and continuous resonance sweep and with the assumption that full active neutrino equilibration obtains ($L_{\nu_e} = L_{\nu_\mu} = L_{\nu_\tau}$).

It is obvious from Eq. (28) that there is a maximum value of the initial potential lepton number for which a solution is obtainable when $\nu_\alpha \rightleftharpoons \nu_s$ is the only operative neutrino flavor conversion channel. This maximum is given by the limit where $\epsilon \to \infty$,

$$\mathcal{L}^{\rm initial}_{\rm max} \approx \frac{3}{4}\frac{F_2\left(\eta_{\nu_\alpha}\right)}{F_2\left(0\right)}. \qquad (29)$$

Scenarios where the bulk of the initial potential lepton number is contained in seas of another flavor of active neutrinos may not allow $\nu_\alpha \rightleftharpoons \nu_s$ conversion to leave a zero final potential lepton number. This is a simple consequence of the post Weak Decoupling conservation of numbers of neutrinos of all kinds. Of course, active-active neutrino flavor transformation in the channels $\nu_\alpha \rightleftharpoons \nu_\beta$ ($\alpha, \beta = {\rm e}, \mu, \tau$) can alter this picture significantly and will be discussed below.

B. Efficiency of Neutrino Flavor Conversion: Adiabaticity

From the previous discussion it is clear that a crucial determinant of the efficiency of active-sterile neutrino flavor conversion at MSW resonances is the adiabaticity of neutrino propagation. It turns out that this is true also for general active-active neutrino mixing in matter. We therefore discuss here the adiabatic character of neutrino flavor evolution in the early universe for both channels.

The causal horizon (particle horizon) is the proper distance traversed by a null signal in the age of the universe

t. In radiation-dominated conditions in the early universe this is

$$d_{\rm H}\left(t\right) = 2t = H^{-1}, \tag{30}$$

where the local Hubble expansion rate is

$$H \approx \left(\frac{8\pi^3}{90}\right)^{1/2} g^{1/2} \frac{T^2}{m_{\rm pl}}. \tag{31}$$

Here $m_{\rm pl} \approx 1.221 \times 10^{22}\,{\rm MeV}$ is the Planck mass. The statistical weight for a relativistic boson species i is $(g_b)_i$, while that for a relativistic fermion species j is $(g_f)_j$. These are related to the total statistical weight g by a sum over all particle species i and j with relativistic kinematics with equilibrium or near equilibrium energy distribution functions and energy densities in the plasma at temperature T, given by $g \equiv \sum_i \left(g_b\right)_i + (7/8)\sum_j \left(g_f\right)_j$. In the epoch between Weak Decoupling and Weak Freeze Out and BBN, photons, $e^{\pm}$ pairs and the active neutrinos are relativistic and appreciably populated so that $g \approx 10.75$ and $t \approx (0.74\,{\rm s})\,(10.75/g)^{1/2}({\rm MeV}/T)^2$. This is a good approximation for the scenarios with net lepton number considered in this paper. This is because the spectral distortions and extra energy density stemming from the net lepton numbers are small effects, causing deviations of the expansion rate from that given above by less than a few percent.

Homogeneity and isotropy in the early universe imply that the entropy in a co-moving volume is conserved. The proper, physical entropy density in radiation-dominated conditions is $S \approx \left(2\pi^2/45\right) g_s T^3$, where g_s is closely related to g and we can take $g_s \approx g$. We can take the co-moving volume element to be the cube of the scale factor a in the Friedman-Lemaitre-Robertson-Walker (FLRW) metric, so that $a^3 S$ is invariant with FLRW time coordinate t and therefore $g^{1/3} aT$ is constant. In turn, this implies that the fractional rate of change of the temperature is related to the expansion rate and the fractional rate of change of the statistical weight by

$$\frac{\dot{T}}{T} \approx -H\left(1 + \frac{\dot{g}/g}{3H}\right). \tag{32}$$

At lower temperatures, where the thermal potential can be neglected, the potential governing neutrino flavor transformation is the difference of the Hamiltonians (*e.g.*, Eq.s (4),(5),(6),(3)) for the transforming neutrino species. For the active-sterile channel $\nu_\alpha \rightleftharpoons \nu_s$, for example, we have defined this potential to be $V = A + B + C$. In the epoch between Weak Decoupling and Weak Freeze Out where the thermal term C is negligible, we have $V \approx H(\nu_\alpha) - H(\nu_s)$. The appropriate potentials for the active-active neutrino flavor transformation channels follow in like manner.

The density scale height for the early universe depends on the neutrino flavor transformation channel and is defined as

$$\begin{aligned} \mathcal{H} &\equiv \left|\frac{1}{V}\frac{dV}{dt}\right|^{-1} \\ &\approx \frac{1}{3}H^{-1}\left|1 + \frac{\dot{g}/g}{3H} - \frac{\dot{\mathcal{L}}/\mathcal{L}}{3H}\right|^{-1}. \end{aligned} \tag{33}$$

Here the approximation on the second line is for active-sterile neutrino flavor transformation and follows on neglecting the thermal potential C and using Eq. (32). When the statistical weight and the lepton numbers are not changing rapidly the density scale height is roughly a third of the horizon scale. This is $\sim 10^5\,{\rm km}$ at the epoch we are considering here.

Define $\Delta \equiv \delta m^2/2E_\nu$. It can be shown that the ratio of the difference of the squares of the *effective* masses in matter to twice the neutrino energy is

$$\begin{aligned} \Delta_{\rm eff} &\equiv \frac{\delta m^2_{\rm eff}}{2E_\nu} \\ &\approx \sqrt{\left(\Delta\cos 2\theta - V\right)^2 + \left(\Delta\sin 2\theta + B_{e\tau}\right)^2}, \end{aligned} \tag{34}$$

where θ is the appropriate effective two-by-two vacuum mixing angle and where $V = A + B + C$ is the appropriate potential for the transformation channel. Here $B_{e\tau}$ is the flavor-off diagonal potential as defined in Qian & Fuller 1995 [19]. The flavor basis off-diagonal potential vanishes, $B_{e\tau} = 0$, for any active-sterile mixing channel.

The effective matter mixing angle $\theta_{\rm M}$ for a neutrino transformation channel with potential V and effective vacuum mixing angle θ satisfies

$$\sin^2 2\theta_{\rm M} = \frac{\Delta^2 \sin^2 2\theta \left(1 + 2E_\nu B_{e\tau}/\delta m^2 \sin 2\theta\right)^2}{\left(\Delta\cos 2\theta - V\right)^2 + \Delta^2 \sin^2 2\theta (1 + 2E_\nu B_{e\tau}/\delta m^2 \sin 2\theta)^2}. \tag{35}$$

The effective matter mixing angle for the antineutrinos in this channel, $\bar{\theta}_{\rm M}$, satisfies a an expression which has opposite signs for the potentials B, A, and $B_{e\tau}$, but which is otherwise identical.

The change in the potential required to drop the effective matter mixing from the maximal resonant value

($\theta_{\rm M} = \pi/4$) to a value where $\sin^2 2\theta_{\rm M} = 1/2$ is termed the resonance width and is

$$\delta V \approx \Delta \sin 2\theta \left| 1 + \frac{2E_\nu B_{e\tau}}{\delta m^2 \sin 2\theta} \right|. \tag{36}$$

The physical width in space, or in FLRW coordinate time t, corresponding to this potential width is

$$\begin{aligned} \delta t &= \frac{dt}{dV}\delta V \approx \left| \frac{1}{V}\frac{dV}{dt} \right|^{-1} \frac{\delta V}{V}\Big|_{\rm res} \\ &\approx \mathcal{H} \tan 2\theta \left| 1 + \frac{2E_\nu B_{e\tau}}{\delta m^2 \sin 2\theta} \right|. \end{aligned} \tag{37}$$

The local neutrino oscillation length at resonance is

$$L^{\rm res}_{\rm osc} = \frac{4\pi E_\nu}{\delta m^2_{\rm eff}} = \frac{2\pi}{\Delta_{\rm eff}} \approx \frac{2\pi}{\delta V}, \tag{38}$$

where the latter approximation is good only at resonance. We can define the dimensionless adiabaticity parameter as proportional to the ratio of the resonance width and the neutrino oscillation length at resonance:

$$\begin{aligned} \gamma &\equiv 2\pi \frac{\delta t}{L^{\rm res}_{\rm osc}} \approx \delta t \delta V \\ &\approx \frac{\delta m^2 \mathcal{H}}{2E_\nu} \cdot \frac{\sin^2 2\theta}{\cos 2\theta} \cdot \left| 1 + \frac{2E_\nu B_{e\tau}}{\delta m^2 \sin 2\theta} \right|^2. \end{aligned} \tag{39}$$

This parameter can be evaluated anywhere in the evolution of neutrino flavors, even well away from resonances and it will serve to gauge the degree to which neutrinos tend to remain in mass eigenstates. The Landau-Zener jump probability, assuming a linear change in potential across the resonance width, is $P_{\rm LZ} \approx \exp(-\pi\gamma/2)$, so that it is clear that a large value of the adiabaticity parameter corresponds to a small probability of jumping between mass eigenstate tracks and, hence, efficient flavor conversion at asymptotically large distance (many resonance widths) from resonance.

Folding in the expansion rate in radiation-dominated conditions, using the conservation of co-moving entropy density, and assuming that we can neglect the thermal potential C, we can show that the adiabaticity parameter for neutrino propagation through an active-sterile resonance is

$$\begin{aligned} \gamma &\approx \frac{\sqrt{5}\,\zeta^{3/4}(3)}{2^{1/8}\pi^3} \cdot \frac{\left(\delta m^2\right)^{1/4} m_{\rm pl} G_{\rm F}^{3/4}}{g^{1/2}} \cdot \left[\frac{\mathcal{L}^{3/4}}{\epsilon^{1/4}}\right] \cdot \left[\frac{\sin^2 2\theta}{\cos^{7/4} 2\theta}\right] \cdot \left| 1 + \frac{\dot g/g}{3H} - \frac{\dot{\mathcal{L}}/\mathcal{L}}{3H} \right|^{-1} \\ &\approx \left(\frac{10.75}{g}\right)^{1/2} \cdot \left[\frac{\delta m^2}{1\,{\rm eV}^2}\right]^{1/4} \cdot \frac{1}{\epsilon^{1/4}} \cdot \left[\frac{\mathcal{L}}{0.01}\right]^{3/4} \cdot \left| 1 + \frac{\dot g/g}{3H} - \frac{\dot{\mathcal{L}}/\mathcal{L}}{3H} \right|^{-1} \cdot \left\{ \frac{\sin^2 2\theta}{1.77 \times 10^{-8}} \right\}. \end{aligned} \tag{40}$$

In these expressions $\epsilon = E_\nu/T$ is the scaled energy of a neutrino at resonance in a channel $\nu_\alpha \rightleftharpoons \nu_s$ characterized by the difference of the squares of the appropriate vacuum mass eigenvalues, δm^2. It is obvious from these considerations that neutrino flavor transformation will be efficient at resonance (*i.e.*, $\gamma \gg 1$) over broad ranges of energy for the regime of the early universe between Weak Decoupling and Weak Freeze Out even for very small effective vacuum mixing angle θ.

Eq. (40) shows that two trends can eventually destroy adiabaticity and, therefore, large scale resonant active-sterile neutrino flavor transformation. As active neutrinos are converted $\mathcal{L}$ is reduced and this reduces γ. In turn, the fractional rate of destruction of $\mathcal{L}$ compared with the Hubble parameter can be become significant, especially if $\mathcal{L}$ is small, and this can also reduce γ.

C. Active-active Neutrino Flavor Conversion and Equilibration

Active neutrinos (ν_e,$\bar\nu_e$,ν_μ,$\bar\nu_\mu$,ν_τ,$\bar\nu_\tau$) transforming among themselves on time scales comparable to or shorter than that of the active-sterile conversion channel can alter significantly the scenario for sterile neutrino production given above. This is apt to be the case if active-active neutrino mixing in medium is large and efficient over a broad range of neutrino energies. Active-sterile neutrino flavor conversion tends to be slow because it occurs through MSW resonances and the rate at which these resonances sweep through the neutrino distribution functions is determined by the expansion of the universe, a slow gravitational time scale.

Coherent neutrino flavor conversion in active-active channels in the early universe can be dominated by the flavor off-diagonal potential. Large in-medium mixing angles can accompany the synchronization seen in calculations of active-active mixing in supernovae and the early universe [13]. If active-active neutrino flavor trans-

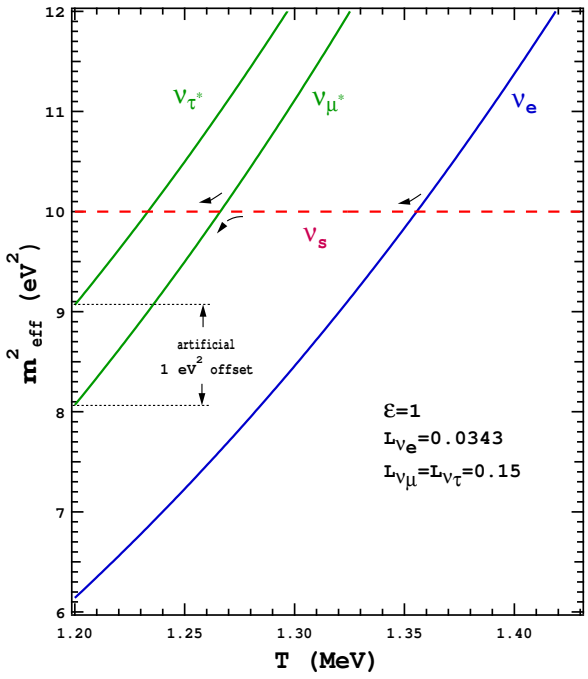

FIG. 3: Level crossing diagram for the case with lepton numbers as shown and for scaled neutrino energy $\epsilon = 1$. The vacuum mass-squared eigenvalue for the (mostly) sterile state is taken as $m_4^2 = 10\,\mathrm{eV}^2$. This is shown as the dashed curve labeled ν_s. An artificial (exaggerated) $1\,\mathrm{eV}^2$ offset between the vacuum mass-squared eigenvalues m_2^2 and m_3^2 has been added so that the curves labeled with ν_μ^* and ν_τ^* are separated for clarity. In reality, the top curve should be split from the lower curve by $\delta m^2 \approx 3 \times 10^{-3}\,\mathrm{eV}^2$. Conversion in the channel $\nu_e \to \nu_s$ is as described in the text.

formation is efficient, then lepton numbers in different active neutrino species can be quickly equilibrated, meaning instantaneous equal lepton numbers.

The flavor diagonal neutrino forward scattering potential in an active-active channel $\nu_\alpha \rightleftharpoons \nu_\beta$ is $A + B = H(\nu_\alpha) - H(\nu_\beta)$. If there is an initial disparity in lepton number in these two flavors then matter-enhanced or -suppressed transformation will go in the direction of reducing this disparity. Though initially the flavor off-diagonal potential $B_{e\tau} \approx 0$, as soon as flavor transformation begins this potential comes up.

The interplay of matter-enhanced coupled active-sterile and active-active neutrino flavor transformation can be complicated and difficult to follow numerically. The size of the debit in the ν_e or $\bar{\nu}_e$ distributions, *i.e.*, the final value of ϵ or $\epsilon_{\rm max}$, may be much more complicated in the general 4×4 case than the scenario outlined above for simple 2×2 $\nu_\alpha \rightleftharpoons \nu_s$ interconversion. We can, however, identify a few cases where we can at least outline the course of neutrino flavor conversion as the universe expands and cools. We will therefore consider two limits: (1) no active-active mixing; and (2) efficient active-active mixing that guarantees that lepton numbers in active species are always the same (instantaneous equilibration).

D. Inefficient Active-Active Neutrino Flavor Conversion

Consider first the case where we neglect active-active neutrino mixing effects. In this case we could have initial lepton numbers that are not fully equilibrated. For example, we could have a scenario where initially $L_{\nu_e} < L_{\nu_\mu} = L_{\nu_\tau}$. In this case the ν_μ and ν_τ experience the largest effective potentials, and hence have the largest effective masses at a given temperature (epoch) in the early universe. Therefore, the first (highest temperature) resonance occurs for ν_s with ν_e, as illustrated in Fig. (3). This resonance will destroy lepton number, as will the subsequent $\nu_\mu^* \rightleftharpoons \nu_s$ resonance, and it will leave a distorted ν_e spectrum.

Here we follow Ref. [20] and define linear combinations of the muon and tauon neutrino flavor states

$$|\nu_\nu^*\rangle \equiv \frac{|\nu_\mu\rangle - |\nu_\tau\rangle}{\sqrt{2}} \tag{41}$$

$$|\nu_\tau^*\rangle \equiv \frac{|\nu_\mu\rangle + |\nu_\tau\rangle}{\sqrt{2}}. \tag{42}$$

This reduces the 4×4 mixing problem of three active neutrinos and a sterile neutrino into a 3×3 problem with $|\nu_\tau^*\rangle$ decoupled (a mass eigenstate in vacuum with no mixing with the other neutrinos). This reduction in dimensionality of the neutrino mixing problem works in vacuum only if the muon and tauon neutrinos are maximally mixed. It also will be valid in medium only if, additionally, these two neutrino flavors experience identical matter interactions. This latter condition is met if $L_{\nu_\mu} = L_{\nu_\tau}$. This symmetry condition will be respected so long as muon and tauon neutrinos behave and transform identically. Indeed, the second resonance encountered as the universe cools, $\nu_\mu^* \rightleftharpoons \nu_s$, respects this condition as the $|\nu_\mu^*\rangle$ state consists of equal parts muon and tauon states.

The sterile neutrinos produced through the $\nu_e \to \nu_s$ resonance are subsequently transformed into ν_μ^* at the second resonance at lower temperature, as depicted for a particular set of initial lepton numbers in Fig. (3). This resonance also converts the ν_μ^* into the sterile state, so that the final abundance of sterile neutrinos results from the conversion of neutrinos which were originally in the ν_μ and ν_τ distributions. Since these distributions have higher lepton number than resides in the $\nu_e/\bar{\nu}_e$ seas, the final number density of sterile neutrinos will be larger than the number of ν_e missing from the ν_e-distribution. As we will see, this case may be more likely to be in conflict with massive neutrino dark matter constraints.

If we temporarily ignore the effect of active-active neutrino flavor transformations, then we can make some general statements about the change in the lepton numbers and ϵ for the ν_e or $\bar{\nu}_e$ distributions in this case of unequal L_{ν_e} and $L_{\nu_\mu} = L_{\nu_\tau}$. If the potential lepton number for electron flavor neutrinos $\mathcal{L}_e$ is driven to zero first then the

changes in the individual active neutrino lepton numbers must be related by

$$2\Delta L_{\nu_e} + \Delta L_{\nu_\mu^*} = -\mathcal{L}_e^{\rm initial}, \quad (43)$$

where here $L_{\nu_\mu^*} = \left(L_{\nu_\mu} + L_{\nu_\tau}\right)/2$, and $\Delta L_{\nu_e} = \Delta n_{\nu_e}/n_\gamma$ and $\Delta L_{\nu_\mu} = \Delta n_{\nu_\mu}/n_\gamma$.

Of course, if $\mathcal{L}_e$ is driven to zero before $\mathcal{L}_\mu^*$, then conversion of ν_e's at the first resonance will cease while conversion in the channel $\nu_\mu^* \to \nu_s$ continues until $\mathcal{L}_{\mu^*}$ is reduced to zero. This will leave $\mathcal{L}_e < 0$ which will result in anti-electron neutrino transformation $\bar\nu_e \to \bar\nu_s$, leaving a non-thermal deficit in the $\bar\nu_e$ distribution.

This is temporary, however. The ν_e potential is zero at the point where $\mathcal{L}_e$ first vanishes. Thereafter, with reduction in $\mathcal{L}_{\mu^*}$, the ν_e potential's magnitude first increases, but then decreases with the expansion of the universe (see Eq. 14). Therefore, the $\bar\nu_s$'s created resonantly via $\bar\nu_e \to \bar\nu_s$ are subsequently re-converted to active neutrinos via a second resonance where $\bar\nu_s \to \bar\nu_e$. This is directly analogous to the re-conversion of $\bar\nu_s$ neutrinos in neutrino-heated outflow in supernovae [21].

In this scenario it is the mu and tau neutrinos, ultimately, that are converted to sterile neutrinos so that the numbers and kinds of converted active neutrinos are given by

$$\mathcal{L}_{\mu^*}^{\rm init} \approx \frac{2}{n_\gamma}\left(\Delta n_{\nu_\mu^*} + \Delta n'_{\nu_\mu^*}\right) - \frac{1}{n_\gamma}(\Delta n_{\nu_e} + \Delta n_{\bar\nu_e}), \quad (44)$$

where $\Delta n_{\nu_\mu^*}$ and $\Delta n'_{\nu_\mu^*}$ are the number of ν_μ^* neutrinos converted before and after $\mathcal{L}_e$ first vanishes, respectively. Likewise, Δn_{ν_e} electron neutrinos are converted before $\mathcal{L}_e$ first vanishes and $\Delta n_{\bar\nu_e}$ electron antineutrinos afterward, though these $\bar\nu_e$'s are eventually returned to the distribution.

There is an additional complication: in the case that all three lepton numbers are equal, the mass-squared differences between the active states are approximately given by their vacuum values, which are quite small. The three resonances depicted in Fig. (3) will then be very close together, and in fact may overlap if the resonance width is sizable.

If the resonances do not overlap, the lepton number destroying resonance will take place between ν_1 and ν_s, where ν_1 is the lightest neutrino mass eigenstate. Since ν_1 has a large ν_e component, this will leave a non-thermal ν_e distribution, and in addition there will be smaller non-thermal distortions of the ν_μ and ν_τ spectra. In the case that the resonances do overlap, the full details of the evolution will be quite complicated, but a similar outcome is obtained nonetheless. To summarize, in all cases a non thermal ν_e spectrum results.

E. Efficient Active-Active Mixing: Instantaneously Equilibrated Lepton Numbers

Let us now consider the limit where in addition to the active-sterile MSW transitions, oscillations/transformations between/among the three active neutrinos occur simultaneously and are efficient. If active-active mixing among all the active flavors is instantaneous and efficient then we only need to consider the case where the lepton numbers are equal, $L_e = L_\mu = L_\tau$, both initially and as active-sterile transformation proceeds. It has been shown that large angle mixing between the three active neutrino species results in the system being driven toward such an equilibrated state [13] at a temperature of $T \gtrsim 2$ MeV.

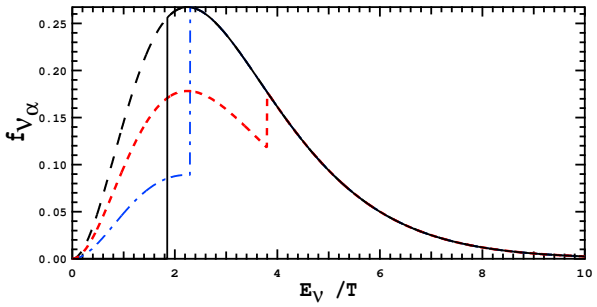

FIG. 4: Final active neutrino energy distribution function f_{ν_α} for Cases 1 (solid line), 2 (short dashed line), and 3 (dot-dash line) in the instantaneous active-active mixing limit as described in the text. Here $\alpha = {\rm e}, \mu, \tau$: all species have the same distribution function. The long-dash line shows the original thermal distribution function common to all active flavors. The particular scenario shown here has $L_{\nu_e} = L_{\nu_\tau} = L_{\nu_\mu} = 0.1$, so that $\epsilon_1 \approx 3.8$, $\epsilon_2 \approx 2.3$, and $\epsilon_3 \approx 1.85$

An obvious additional effect of efficient active-active oscillations will be to partially refill any hole that was left in the ν_e distribution. It is important to note, though, that this refilling cannot be complete. For maximal $\nu_e - \nu_{\mu,\tau}$ mixing, the hole in the distribution can be only partially refilled. In vacuum the measured solar neutrino mixing angle is less than maximal, $\theta_{\rm solar} \simeq 32.5^\circ$, and U_{e3} is relatively small. In medium, at best we will obtain maximal matter mixing angles in the limit where the flavor off-diagonal potential is large. We again therefore expect about 0 to 2/3 refilling at most, so that a non-thermal ν_e spectrum is always obtained by the epoch of Weak Freeze Out. Even if it were somehow possible for the resonance to effectively involve only ν_s and ν_μ/ν_τ, active-active oscillations would again act to refill the hole in the resulting non thermal ν_μ and/or ν_τ spectra, and in so doing create a non-thermal ν_e distribution.

We can identify three cases.

Case 1: We have only one sterile neutrino species and only one channel for its production, $\nu_\alpha \to \nu_s$. If this channel is, *e.g.*, $\nu_e \to \nu_s$, then the neutrinos in the ν_τ and ν_μ distributions will, in the limit of instantaneous maximal mixing, partially fill in the hole left by the active-sterile conversion process. Given the boundary condition of equal lepton numbers in all active flavors at all times, the smooth resonance sweep scenario will leave each active neutrino distribution with a low energy "hole" with

2/3 of the normal population out to some value of scaled neutrino energy ϵ_1. In terms of the initial potential lepton number $\mathcal{L}^{\rm init} = \mathcal{L}_e = \mathcal{L}_\mu = \mathcal{L}_\tau$, this is obtained by solving the integral equation

$$2\mathcal{L}^{\rm init} \approx \frac{1}{F_2\left(0\right)} \int_0^{\epsilon_1} \frac{x^2 dx}{e^{x-\eta}+1}. \tag{45}$$

In this scenario the number of active neutrinos converted in each flavor are equal ($\Delta n_\nu \equiv \Delta n_{\nu_e} = \Delta n_{\nu_\mu} = \Delta n_{\nu_\tau}$) and this, in turn, is equal to the number of sterile neutrinos produced n_s,

$$\frac{n_s}{n_\gamma} \approx \frac{\Delta n_\nu}{n_\gamma} \approx \frac{3}{4}\mathcal{L}^{\rm init}. \tag{46}$$

Up until now, we have been working under the assumption that the sterile neutrino takes part in a resonance with one of the active neutrino flavors, ν_α, taken to be ν_e. However, if the initial lepton numbers are equal, the resonance will instead occur between ν_s and a superposition of the three active neutrinos. In principle, all three of the active neutrinos may mix with the sterile, so the MSW resonance which is responsible for lepton number destruction may occur for the sterile neutrino and a linear superposition of the three active neutrinos. For example, in the so called "3+1" LSND inspired mixing scheme, both θ_{14} and θ_{24} are required to be non-zero, and the sterile effectively mixes with all three active neutrinos (as there will also be indirect $\nu_\tau - \nu_s$ mixing).

Furthermore, if there is one light sterile neutrino, there may be others. In fact it has been claimed that two sterile species are a better fit to the LSND data than just one [26]. So this suggests Cases 2 and 3.

Case 2: Allow two channels of sterile neutrino production and two kinds of light sterile neutrinos ν_{s1} and ν_{s2}. As an example, we could have $\nu_e \rightarrow \nu_{s1}$ and $\nu_\mu \rightarrow \nu_{s2}$, but again with instantaneous mixing among all the active neutrino flavors. A smooth resonance sweep scenario will leave each active neutrino distribution with a low energy hole now with 1/3 of the normal population out to some value of scaled neutrino energy ϵ_2. In terms of the initial potential lepton number $\mathcal{L}^{\rm init} = \mathcal{L}_e = \mathcal{L}_\mu = \mathcal{L}_\tau$, this is obtained by solving the integral equation

$$\mathcal{L}^{\rm init} \approx \frac{1}{F_2\left(0\right)} \int_0^{\epsilon_2} \frac{x^2 dx}{e^{x-\eta}+1}. \tag{47}$$

In this scenario the number of active neutrinos converted in each flavor are equal ($\Delta n_\nu \equiv \Delta n_{\nu_e} = \Delta n_{\nu_\mu} = \Delta n_{\nu_\tau}$) and this, in turn, is equal to 1/2 the number of sterile neutrinos produced n_s,

$$\frac{n_s}{n_\gamma} \approx \frac{2\Delta n_\nu}{n_\gamma} \approx \frac{3}{4}\mathcal{L}^{\rm init}. \tag{48}$$

For a given initial potential lepton number, this is the same total number of sterile neutrinos (of all kinds) produced as in Case 1. Though there are now two channels for ν_s production, ϵ_2 is smaller than ϵ_1. In Case 1 ϵ_1 is relatively larger because as ν_e's are converted to steriles two active neutrino distributions compensate by feeding neutrinos into the hole, forcing the resonance to sweep further (higher in energy) through the ν_e distribution to erase the net lepton numbers. In Case 2 only one active neutrino distribution remains to compensate for the hole.

Case 3: Allow all three active neutrinos to convert simultaneously to three kinds of light sterile neutrinos ν_{s1}, ν_{s2}, ν_{s3}. Now a smooth resonance sweep scenario will leave each active neutrino distribution with a low energy hole with *zero* population out to some value of scaled neutrino energy ϵ_3. In terms of the initial potential lepton number $\mathcal{L}^{\rm init} = \mathcal{L}_e = \mathcal{L}_\mu = \mathcal{L}_\tau$, this is obtained by solving the integral equation

$$\frac{2}{3}\mathcal{L}^{\rm init} \approx \frac{1}{F_2\left(0\right)} \int_0^{\epsilon_3} \frac{x^2 dx}{e^{x-\eta}+1}. \tag{49}$$

In this scenario the number of active neutrinos converted in each flavor are equal ($\Delta n_\nu \equiv \Delta n_{\nu_e} = \Delta n_{\nu_\mu} = \Delta n_{\nu_\tau}$) and this, in turn, is equal to 1/3 the number of sterile neutrinos produced n_s,

$$\frac{n_s}{n_\gamma} \approx \frac{3\Delta n_\nu}{n_\gamma} \approx \frac{3}{4}\mathcal{L}^{\rm init}. \tag{50}$$

This is the same number of sterile neutrinos produced as in Cases 1 and 2 for a given $\mathcal{L}^{\rm init}$. This result comes about for the same reasons indicated in the last paragraph. Note that $\epsilon_1 > \epsilon_2 > \epsilon_3$ for a given initial potential lepton number in each of our three cases.

For Cases 1, 2, and 3 the active neutrino distribution functions will be left with population deficits relative to the thermal case. This is shown in Fig. (4) for the particular scenario where each active flavor starts out with lepton number $L_{\nu_e} = L_{\nu_\tau} = L_{\nu_\mu} = 0.1$. Solving the above equations for the three cases yields $\epsilon_1 \approx 3.8$, $\epsilon_2 \approx 2.3$, and $\epsilon_3 \approx 1.85$ in this example.

In obvious fashion all of the above discussion applies to $\bar{\nu}_s$ production if the initial lepton numbers are negative. We should also note that the actual active and sterile neutrino energy distributions in all of the limits considered here may differ considerably from those shown in the figures, particularly if the smooth and continuous resonance sweep approximation does not apply. In this case, the resulting neutrino energy distribution functions may have deficits extending to higher energy but arranged in a "picket fence" character. We conclude that a sterile neutrino in the mass range of interest is almost certain to leave non-thermal active neutrino distribution functions if the lepton number is significant.

III. CONSTRAINTS ON STERILE NEUTRINOS AND LEPTON NUMBERS

The entire plausible range of sterile neutrino masses and net lepton numbers of interest is not likely to be consistent with all of the current observational bounds.

For example, we may demand that the initial net lepton numbers are large enough to suppress the production of fully thermalized seas of ν_s and $\bar{\nu}_s$. Eq. (2) shows that the lepton number necessary for suppression of thermal sterile neutrino production depends both on neutrino mass and neutrino average energy. We will hold off on considering BBN effects/limits until the next section.

As discussed in the introduction, a population of sterile neutrinos could provide enough relativistic energy density, depending again on sterile neutrino mass, to run afoul of large scale structure/CMB bounds [8]. The above-cited analysis of the SDSS data [10] using CMB anisotropy limits, galaxy clustering and bias, and coupled with the matter power spectrum inferred from the Lyman-alpha forest suggest a limit on the neutrino mass of 0.79 eV (95% CL). This corresponds to a limit on the neutrino closure fraction

$$\Omega_\nu^{\rm lim} h^2 < 0.0084 \ (95\%\,{\rm CL}), \tag{51}$$

where h is the Hubble parameter at the current epoch in units of $100\,{\rm km\,s^{-1}\,Mpc^{-1}}$. This is comparable to the older WMAP bound, $\Omega_\nu^{\rm lim} h^2 < 0.0076$ (95% CL). However, the Eq. (51) bound is more appropriate here as it assumes a "3+1" neutrino mass scenario in contrast to the three neutrinos with a common mass assumed in the WMAP analysis. Adopting the Eq. (51) bound suggests that thermal distributions of ν_α and $\bar{\nu}_\alpha$ neutrinos are acceptable only if they have rest masses

$$m_{\nu_\alpha} \lesssim 0.79\,{\rm eV}\left[\frac{2F_2\,(0)}{F_2\,(\eta_{\nu_\alpha}) + F_2\,(-\eta_{\nu_\alpha})}\right]\left[\frac{\Omega_\nu^{\rm lim} h^2}{0.0084}\right], \tag{52}$$

where $\alpha = {\rm e}, \mu, \tau, {\rm s}$. We can connect this with the a putative thermal sterile neutrino sea by noting that $m_{\nu_s} \approx \left(\delta m^2_{\rm as}\right)^{1/2}$. So, for example, $\delta m^2_{\rm as} > 0.63\,{\rm eV}^2$ is disallowed if all the sterile neutrino species have thermal distributions. This would eliminate much of the LSND-inspired sterile neutrino mass range.

However, the coherent sterile neutrino production scenarios discussed above may do better at creeping in under the closure contribution bound. For one thing, only ν_s (or $\bar{\nu}_s$) and not its opposite helicity partner are produced coherently. Furthermore, the sterile neutrinos are produced in numbers of order the initial lepton number. This will be smaller than a general thermal population.

At the epoch of coherent sterile neutrino production the ratio of the number of active neutrinos Δn_{ν_α} converted to steriles to the number total density of a thermal distribution of ν_α plus $\bar{\nu}_\alpha$ neutrinos is in the ratio of the closure contributions of a sterile species to thermal neutrino species:

$$\frac{\Omega_s h^2}{\Omega^{\rm therm}_{\nu_\alpha + \bar{\nu}_\alpha} h^2} \approx R_s \equiv \frac{N_s \Delta n_{\nu_\alpha}}{n_{\nu_\alpha} + n_{\bar{\nu}_\alpha}}, \tag{53}$$

where N_s is the number of active-sterile mixing channels operating in the production of sterile neutrinos. In turn

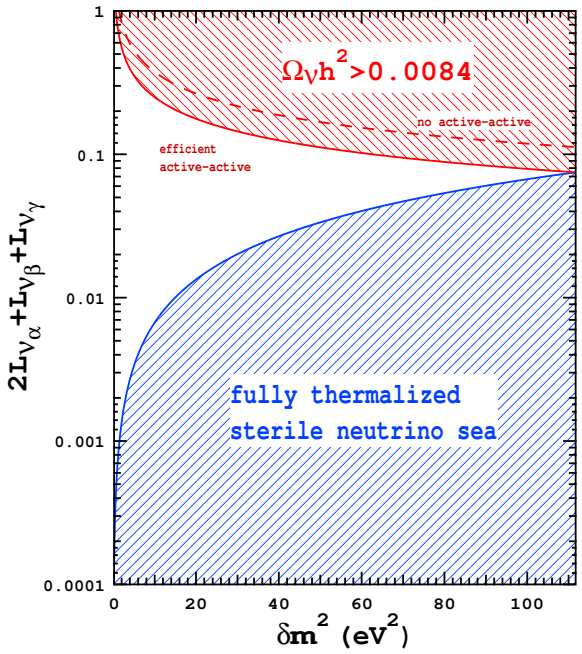

FIG. 5: Constraints on the the ranges of active-sterile mass-squared splitting and potential lepton number as derived in the smooth and continuous resonance sweep limit. Parameter ranges which give sufficient sterile neutrino production to exceed the bound on the neutrino closure fraction are shown cross hatched, as are parameter ranges which allow for complete or nearly complete thermal, undiluted energy distribution functions for a sterile species. The upper solid line is for efficient active-active mixing in Cases 1, 2 , or 3, while the upper dashed line gives the constraint for $\nu_\alpha \to \nu_s$ with no active-active mixing.

it can be shown that

$$R_s \approx \left[\frac{1}{F_2\,(0)}\int_0^\epsilon \frac{x^2}{e^{x-\eta}+1}\right]\left[\frac{F_2\,(0)}{F_2\,(\eta_{\nu_\alpha}) + F_2\,(-\eta_{\nu_\alpha})}\right] \tag{54}$$

where ϵ and the degeneracy parameter η are values consistent with the particular sterile neutrino production scheme. From these relations we can show that

$$\Omega_s h^2 \approx \left(1.062 \times 10^{-2}\right)\left(\frac{\beta}{2}\right)\mathcal{L}\left[\frac{\delta m^2_{\rm as}}{{\rm eV}^2}\right]^{1/2}, \tag{55}$$

where $\mathcal{L}$ is an appropriate potential lepton number and where β is a parameter that is related to the particular sterile neutrino production scheme and the number of active-sterile channels in that scheme. For example, $\beta = 2$ for Cases 1, 2, and 3 of the efficient active-active limit, whereas $\beta = 4/3$ for $\nu_\alpha \to \nu_s$ only with no active-active mixing. All of these constraints are summarized in Fig. (5).

IV. NON-THERMAL NEUTRINO ENERGY SPECTRA AND PRIMORDIAL NUCLEOSYNTHESIS

The neutron-to-proton ratio is set by the competition of the expansion rate of the universe and the forward and reverse rates of the following lepton capture/decay processes:

$$\nu_e + n \rightleftharpoons p + e^-, \tag{56}$$

$$\bar{\nu}_e + p \rightleftharpoons n + e^+, \tag{57}$$

$$n \rightleftharpoons p + e^- + \bar{\nu}_e. \tag{58}$$

$$n + e^+ + \nu_e \rightarrow p. \tag{59}$$

In the epoch where the temperature is greater than that of Weak Freeze-Out, $T > T_{\rm wfo}$, the isospin of any nucleon will flip from neutron to proton and back at a rate which is rapid compared to the expansion rate. Even post-Weak-Decoupling, the lepton capture rates on nucleons can be large. This is because the number densities of relativistic neutrinos and charged leptons are some 10 orders of magnitude larger than the baryon density. The neutron-to-proton ratio in the $T > T_{\rm wfo}$ limit has a steady state value given by [22]

$$\begin{aligned} \frac{n}{p} &\approx \frac{\lambda_{\bar{\nu}_e p} + \lambda_{e^- p} + \lambda_{p e \bar{\nu}_e}}{\lambda_{\nu_e n} + \lambda_{e^+ n} + \lambda_{n\ \rm decay} + \lambda_{n e^+ \nu_e}}, \\ &\approx \frac{\lambda_{\bar{\nu}_e p} + \lambda_{e^- p}}{\lambda_{\nu_e n} + \lambda_{e^+ n}}, \end{aligned} \tag{60}$$

where, for example, $\lambda_{\bar{\nu}_e p}$ is the forward rate for the process in Eq. (57), $\lambda_{e^+ n}$ is the corresponding reverse rate, and $\lambda_{n\ \rm decay}$ is the forward rate for the neutron decay process in Eq. (58), while $\lambda_{p e \bar{\nu}_e}$ is the corresponding three body capture reverse rate, and $\lambda_{n e^+ \nu_e}$ is the three body capture process on neutrons. Other notation follows in obvious fashion. The second approximation in Eq. (60) is valid when the three body rates can be neglected.

Eq. (60) is valid in general only when the neutron-to-proton ratio is in strict steady state equilibrium. In fact, the lepton capture rates on free nucleons can be comparable to the expansion rate at Weak Freeze Out. This implies that there is a correction to the Eq. (60) result which depends on the rate of change of the lepton capture rates. This term can be significant. In fact, the neutron-to-proton ratio will continue to change well after Weak Freeze Out. In this sense, our estimated effects of the "holes" in neutrino distribution functions are sometimes likely to be conservative.

As the universe expands and the temperature drops, the relative values of these rates change and, hence, so does the neutron-to-proton ratio. At temperatures $T \geq T_{\rm wfo}$ the three body lepton capture and free neutron decay processes have rates which are unimportant compared to those of the lepton capture rates. For temperatures $T \gg T_{\rm wfo}$, typical lepton energies are large compared to the energy thresholds in the forward rate of the process in Eq. (57) and the reverse rate for the process in Eq. (56), so that if the lepton numbers are small we would have $n/p \approx 1$, or $Y_e \approx 1/2$.

For $T < T_{\rm wfo}$ the lepton capture rates and the three body capture rates eventually become small compared to the expansion rate and the neutron-to-proton ratio will only slowly decrease with time on account of free neutron decay. In standard BBN, $n/p \approx 1/6$ at $T_{\rm wfo} \approx 0.7\,{\rm MeV}$ and has fallen to $n/p \approx 1/7$ at $T_{\rm NSE} \approx 100\,{\rm keV}$, where strong and electromagnetic nuclear interactions begin to freeze out and neutrons are efficiently incorprated into alpha particles.

In fact, the primordial ^{4}He yield is determined roughly by the number of neutrons available at $T_{\rm NSE}$. In mass fraction, this is $X_\alpha \approx 2(n/p)/(n/p+1)$, or 25% for $n/p = 1/7$. The standard BBN ^{4}He mass fraction yield prediction is $24.85 \pm 0.05\%$ using the CMB (Cosmic Microwave Background) anisotropy-determined baryon density [6]. (The baryon closure fraction as derived from the deuterium abundance [23] is consistent with the CMB-derived value.)

The observationally-inferred primordial helium abundance has a long and troubled history. One group pegs this abundance at $0.238 \pm 0.002 \pm 0.005$ [24], while another using similar but not identical compact blue galaxy data estimates 0.2421 ± 0.0021 [25]. These values are quite restrictive. However, these older estimates may now be superseded by more recent analyses as discussed in the Introduction.

A more detailed analysis of the helium and hydrogen emission lines done in Ref. [7] suggests that the allowable range of mass fraction for primordial ^{4}He is 0.232 to 0.258. This is fairly generous compared to previous "limits." However, it is a good bet that a 5% or 10% increase in the calculated, *predicted* yield in ^{4}He would be an unwelcome development. Therefore, as a crude guideline, in this paper we will take a 5% to 10% increase in the steady state equilibrium neutron-to-proton ratio at $T = 0.7\,{\rm MeV}$ as estimated by Eq. (60) as a limit. We emphasize that this is only a rough guide as to when non-thermal neutrino distribution effects are likely unacceptable. Should there be experimental confirmation of the LSND result or other evidence for light sterile neutrinos then our rates, together with the simultaneously followed resonance sweep, will have to be computed along with the nuclear reactions in the primordial nucleosynthesis code.

If the electron neutrinos and antineutrinos and the electrons and positrons all have Fermi-Dirac energy spectra, then Eq. (60) can be reduced to [27, 28]

$$\frac{n}{p} \approx \frac{\left(\lambda_{e^- p}/\lambda_{e^+ n}\right) + e^{-\eta_{\nu_e} + \eta_e - \xi}}{\left(\lambda_{e^- p}/\lambda_{e^+ n}\right) e^{\eta_{\nu_e} - \eta_e + \xi} + 1}, \tag{61}$$

where $\eta_e = \mu_e/T$ is the electron degeneracy parameter and $\xi = (m_n - m_p)/T \equiv \delta m_{np}/T \approx 1.293\,{\rm MeV}/T$ is

the neutron-proton mass difference divided by temperature. Here we have neglected the neutron decay/three-body capture processes of Eq. (58). The expression in Eq. (61) is generally true for Fermi-Dirac leptonic energy distribution functions, even if the neutrinos and electrons/positrons are not in true thermal and chemical equilibrium. If and only if chemical equilibrium *actually* obtains (or did obtain at some early epoch) are we guaranteed to have $\mu_e - \mu_{\nu_e} = \mu_n - \mu_p$, where μ_n and μ_p are the neutron and proton total chemical potentials, respectively, and only in this case does Eq. (61) reduce to

$$\frac{n}{p} \approx e^{(\mu_e - \mu_{\nu_e} - \delta m_{np})/T}. \tag{62}$$

With strict chemical equilibrium and with Fermi-Dirac energy distributions for all leptons, we could conclude from Eq. (62), for example, that a positive chemical potential for electron neutrinos (*i.e.*, an excess of ν_e over $\bar{\nu}_e$) would suppress the neutron-to-proton ratio at Weak Freeze-Out relative to that for $\eta_{\nu_e} = 0$. This behaviour follows also from a straightforward application of Le Chatlier's principle to the processes in Eqs. (56) and (57). A decrease in the neutron abundance translates, in turn, into a decrease in the predicted ^{4}He yield.

However, if after Weak Decoupling the neutrino distribution functions are modified by active-sterile neutrino conversion, $\nu_\alpha \rightleftharpoons \nu_s$, then the resulting active and sterile neutrino distribution functions would not be Fermi-Dirac in character and we could not employ Eq. (62) to determine the neutron-to-protion ratio at $T_{\rm wfo}$. Instead, we would be forced in this case to evaluate and follow the rates directly. We can get a crude estimate of the effects of these altered rates on the neutron-to-proton ratio by using them in Eq. (60).

Let us first consider the modifications of the lepton capture rates for the case where a net lepton number drives conversion of electron neutrinos to singlet neutrinos, $\nu_e \to \nu_s$. Further, for argument's sake, let us assume that the resonant conversion proceeds in a smooth and continuous sweep from low energy toward higher energy in the manner of Eq. (26), *i.e.*, all electron neutrinos with scaled energy less than ϵ are converted to sterile neutrinos.

The result for inefficient active-active cases or for Case 3 of the efficient active-active limit would be a ν_e energy distribution function as in Fig. (1), which is zero for all values of scaled neutrino energy $0 \leq E_{\nu_e}/T \leq \epsilon$, and has a conventional Fermi-Dirac thermal distribution character for neutrino energies $E_{\nu_e}/T > \epsilon$. The non-thermal energy spectrum for ν_e in this case will alter the rates for electron capture on protons, $e^- + p \to n + \nu_e$, and for ν_e capture on neutrons, $\nu_e + n \to p + e^-$, over what these rates would have been prior to $\nu_e \to \nu_s$ conversion. Because there are now *fewer* ν_e's, the electron capture on proton reaction will be less Fermi blocked and, hence, the capture rate, λ_{e^-p}, will be larger. By the same token, fewer ν_e's will translate into a reduction of the ν_e capture rate on neutrons, $\lambda_{\nu_e n}$. Note that both a larger value for λ_{e^-p} and a smaller value for $\lambda_{\nu_e n}$ go in the direction of *increasing* the neutron-to-proton ratio in weak steady state equilibrium. This is obvious from Eq. (60).

For a quantitative gauge of the effects of these altered lepton capture rates, let us consider a particular active-sterile neutrino conversion scenario in the channel $\nu_e \to \nu_s$. We can get an idea of how important these effects might be if we take each of the three neutrino flavors to have a lepton number near or at the maximum allowed. Therefore, take $L_{\nu_\mu} = L_{\nu_\tau} = 0.15$, corresponding to degeneracy parameters $\eta_{\nu_\mu} = \eta_{\nu_\tau} \approx 0.219$, and take $L_{\nu_e} \approx 0.0343$, corresponding to electron neutrino degeneracy parameter $\eta_{\nu_e} = 0.05$. This will give an initial potential lepton number in the $\nu_e \to \nu_s$ transformation channel,

$$\mathcal{L}_e^{\rm initial} = 2L_{\nu_e} + L_{\nu_\mu} + L_{\nu_\tau} \approx 0.368. \tag{63}$$

In this case the difference in neutrino energy density over the zero lepton case is only 0.2%. Therefore, the expansion rate of the universe at Weak Freeze Out in this case will differ from the standard BBN model by only $\sim 0.2\%$. Therefore, the expansion rate by itself would give a negligible difference in neutron-to-proton ratio between the case with the lepton number in Eq. (63) and the zero lepton number, standard BBN case.

However, positive electron lepton number in this case, corresponding to $\eta_{\nu_e} = 0.05$, would by itself, with no $\nu_e \to \nu_s$ conversion, result in a significant reduction in the neutron-to-proton ratio and a concomitant reduction in the ^{4}He yield over the standard BBN case. If we use the above rates and Eq. (60) we can estimate that the zero lepton number, standard case gives a neutron-to-proton ratio at Weak Freeze Out at temperature $T = 0.7\,{\rm MeV}$,

$$\left.\frac{n}{p}\right|_{\epsilon=0}^{\eta_{\nu_e}=0} \approx 0.159, \tag{64}$$

or roughly 1 to 6 as discussed above.

By contrast, if we again allow no neutrino conversion (equivalently, $\epsilon = 0$), but now include the electron neutrino degeneracy $\eta_{\nu_e} = 0.05$, we obtain for the neutron-to-proton ratio at Weak Freeze Out, $T = 0.7\,{\rm MeV}$,

$$\left.\frac{n}{p}\right|_{\epsilon=0}^{\eta_{\nu_e}=0.05} \approx 0.151. \tag{65}$$

This is a $\sim$ 5% drop in the neutron-to-proton ratio and would imply a comparable drop in the ^{4}He yield. It has been argued that an electron neutrino degeneracy of this order is actually the best fit to some of the observationally-determined primordial helium abundance values [14].

Assuming a smooth and continuous resonance sweep through the ν_e distribution, we can employ Eq. (25) and solve for the value of ϵ that gives zero final potential lepton number $\mathcal{L}_e = 0$. In this case $\epsilon \approx 2.724$. Using the estimates for the lepton capture rates given in Appendix A

with $\epsilon = 2.724$ suggests that the neutron-to-proton ratio at Weak Freeze Out ($T = 0.7\,\mathrm{MeV}$) for the case with the lepton numbers in Eq. (63), and where we allow for ν_e conversion to steriles, is

$$\left.\frac{n}{p}\right|_{\epsilon=2.724}^{\eta_{\nu_e}=0.05} \approx 0.174. \tag{66}$$

Note that this represents a $\sim 9\%$ *increase* in the neutron-to-proton ratio and, hence, the ^{4}He yield over the standard BBN case. Furthermore, this result is a $\sim 15\%$ increase in n/p over the no-transformation case with a neutrino degeneracy parameter, Eq. (65). We could conclude that these lepton numbers are likely not a way to make the LSND result consistent with BBN, especially given the current tension between the observationally-inferred primordial helium abundance and the ^{4}He yield predicted by standard BBN.

However, as discussed above, the resonance may not sweep smoothly and continuously all the way to the point where the potential lepton number has been driven to zero and neutrino flavor evolution through resonance ceases to be adiabatic. In fact, the adiabatic conversion and smooth resonance sweep in the channel $\nu_e \to \nu_s$ may cease at $\epsilon_{\rm max}$, as outlined in the last section. There are two possibilities from this point onwards.

First, it is possible that the resonance sweep for scaled energy values beyond the maximum, $\epsilon > \epsilon_{\rm max}$, is accompanied by non-adiabatic neutrino flavor evolution. That is, neutrino flavor conversion ceases at $\epsilon_{\rm max}$. The deficit in the ν_e distribution function would be smaller in this case and, consequently, the modifications in the rates would be smaller as well. For the specific example case discussed above with overall potential lepton number $\mathcal{L}_e = 0.368$, we can estimate that $\epsilon_{\rm max} \approx 1.46$. This gives a much smaller increase in the neutron-to-proton ratio over the no flavor conversion case,

$$\left.\frac{n}{p}\right|_{\epsilon_{\rm max}=1.46}^{\eta_{\nu_e}=0.05} \approx 0.156. \tag{67}$$

This result lies between the no conversion case with neutrino degeneracy, Eq. (65), and the zero degeneracy, no conversion case in Eq. (64). Therefore, in this scenario a sterile neutrino with the LSND parameters *could* be reconciled with the predictions of BBN and the observationally-inferred primordial abundance of helium.

By contrast, the second possibility for resonance sweep beyond $\epsilon_{\rm max}$ likely would preclude a much larger range of lepton number as a means for reconciling BBN and an "LSND" sterile neutrino species. In this second resonance sweep scenario, there would be sporadic adiabatic conversion $\nu_e \to \nu_s$ for $\epsilon > \epsilon_{\rm max}$ until the potential lepton number is driven to zero. This would imply that, in addition to the hole in the ν_e distribution function for $\epsilon < \epsilon_{\rm max}$, there would now be occasional holes with zero population for short intervals in scaled energy in the region $\epsilon > \epsilon_{\rm max}$. The ν_e distribution function in this case would have a "picket fence" character for $\epsilon > \epsilon_{\rm max}$.

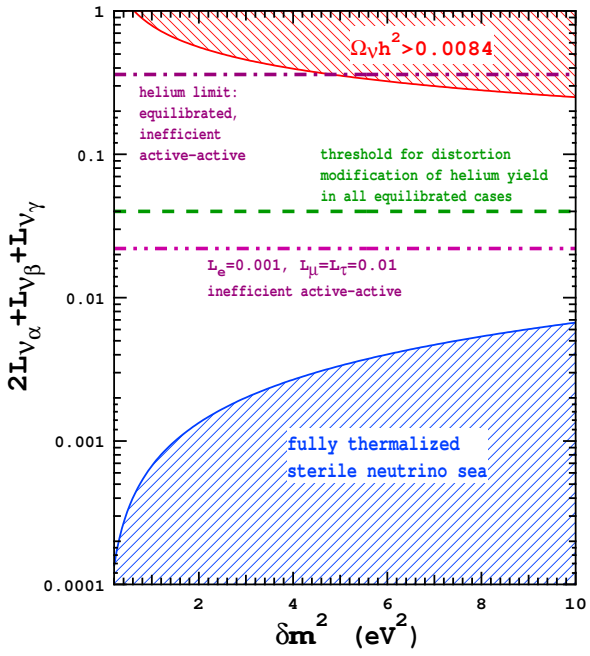

FIG. 6: Constraints as in Fig. (5) and now with BBN "guidelines," see text. The double-dot-dashed line gives an estimate of the limiting ^{4}He yield in a no active-active mixing scenario where $L_e = 0.001$ and $L_\mu = L_\tau = 0.01$. The dashed line gives a threshold in potential lepton number for all cases where neutrino lepton numbers are equilibrated, including those with efficient active-active mixing. Beyond this threshold there are significant alterations in the helium yield stemming from non-thermal neutrino distributions. The upper dash-dot line gives a rough estimate of the limiting potential lepton number for equilibrated cases with inefficient active-active mixing.

Removing ν_e's from the distribution at higher energies would result in a much greater decrease in $\lambda_{\nu_e n}$ and a greater increase in $\lambda_{e^- p}$ for a given initial potential lepton number than in the case with a smooth resonance sweep. In turn, this would imply a larger overall increase in the neutron-to-proton ratio than for the smooth sweep scenario. The reason for the greater rate modifications in this case is that the integrands of the lepton capture rate expressions scale like the fourth power of lepton energy (see Appendix A). Both the weak cross sections and the neutrino fluxes are larger at higher neutrino energies.

Similar arguments apply to the cases where active-active neutrino mixing is efficient and neutrino lepton numbers equilibrate rapidly. However, in Cases 2 and 3 discussed above, the neutrino populations in the "hole" are not zero, with the consequence that for a given ϵ value the rates are not as affected as in the cases discussed above. For example, for initial lepton numbers $L_{\nu_e} = L_{\nu_\mu} = L_{\nu_\tau} = 0.1$, corresponding to $\eta_{\nu_e} \approx 0.146$, the standard lepton degenerate Weak Freeze Out neutron-to-proton ratio would be $n/p \approx 0.136$, which would correspond to an unacceptably low ^{4}He yield. By contrast, when we allow sterile neutrino production in Case 1, the

resulting non-thermal ν_e spectrum increases this ratio to ≈ 0.15, an allowed value. In Case 2 this goes to 0.145 while in Case 3 it is 0.144, each likely allowed if somewhat low. Taking all the initial lepton numbers equal to 0.15 (*i.e.*, $\mathcal{L} = 0.6$), an utterly disallowed proposition without neutrino spectral distortion, yields a acceptable n/p-ratio for Cases 1 and 2.

Figures of merit for these considerations and potential lepton number and BBN-effects "guidelines" are shown in Fig. (6). The horizontal lines and the corresponding labels are meant to give a guide as to the effects of various assumed initial lepton numbers on the neutron-to-proton ratio and ^{4}He yield as discussed above.

However, these BBN effects lines (guidelines) in our figures are to be regarded only as quite rough estimates of where non-thermal effects need to be considered. The guidelines are crude for three principal reasons. (1) MSW resonance scaled energy ϵ is proportional to δm^2 and inversely proportional to the product of T^4 and the instantaneous value of $\mathcal{L}$ (see Eq. 15), so that the cases with the lowest values of δm^2 and larger values of $\mathcal{L}$ on the plot may not experience the full resonance sweep required to deplete all of the initial lepton number prior to reaching the Weak Freeze Out temperature. This would result in a reduced alteration in lepton capture/decay rates at Weak Freeze Out. (2) Likewise, the cases with the highest values of δm^2 coupled with lower values of $\mathcal{L}$ on the plot may already have experienced considerable resonant active-sterile conversion and concomitant lepton number depletion *before* Weak Decoupling, while neutrino scattering was still effective. This would either wash out much of the "hole" in the neutrino distribution functions or leave a hole of reduced energy width at higher energies. (3) The neutron-to-proton ratio actually changes in response to altered lepton capture/decay rates well after Weak Freeze Out, as discussed above.

In any case, we do not know precisely the Weak Decoupling temperature and, as we have emphasized, Weak Freeze Out is not really an instantaneous occurrence. Furthermore, we may not have the smooth resonance sweep scenario, but rather something more akin to the "picket fence" neutrino distribution functions discussed above. All of this implies that the magnitude of the above effects are hard to gauge quantitatively without a fully coupled and simultaneous calculation of nuclear and weak reactions and resonance sweep/lepton number depletion. Nevertheless, we believe that our BBN guidelines at least indicate where the existence of light sterile neutrinos and concomitant non-thermal distribution function and weak rate effects may alter BBN significantly.

What about conversion of anti-electron neutrinos to singlets, $\bar{\nu}_e \to \bar{\nu}_s$? This process can be matter-enhanced when the overall potential lepton number is negative, $\mathcal{L}_e < 0$. It will be exactly analogous to the positive potential lepton number case, at least as far as the neutrino flavor conversion and the resonance sweep physics goes. The close analogy ends, however, when it comes to the lepton capture reactions.

If the resonance sweeps adiabatically out to a scaled antineutrino energy $\bar{\epsilon}$, a hole will be left in the $\bar{\nu}_e$ distribution, in complete analogy to the cases discussed above. Fewer $\bar{\nu}_e$'s will translate into a decreased antineutrino capture rate, $\bar{\nu}_e + p \to n + e^+$, and an increased rate of positron capture, $e^+ + n \to p + \bar{\nu}_e$. These rate modifications both go in the direction of decreasing the neutron-to-proton ratio n/p at weak Freeze Out, as is obvious from Eq. (60). Production of $\bar{\nu}_e$'s with efficient active-active neutrino mixing follow schemes in obvious analogy to the cases discussed in this limit with positive potential lepton number.

One might think at first that simply changing the sign of the potential lepton numbers given in the above examples could result in a suppressed n/p and, therefore, no BBN conflict with a large lepton number scenario for reconciling observed abundances with an LSND sterile state. This is not correct however, because the threshold in the reaction $\bar{\nu}_e + p \to n + e^+$ plays a crucial role. As can be seen in the rate integrals given in Appendix A, in this channel a $\bar{\nu}_e$ must have an energy in excess of the threshold, $E_{\bar{\nu}_e} > E^{\rm thresh}_{\bar{\nu}_e}$ to be captured. The threshold is $E^{\rm thresh}_{\bar{\nu}_e} = Q_{np} + m_e c^2 \approx 1.804\,{\rm MeV}$.

Consider the smooth resonance sweep scenario outlined above where $\bar{\nu}_e$'s are converted to sterile states up to scaled energy $\bar{\epsilon}$. Unless $\bar{\epsilon} > E^{\rm thresh}_{\bar{\nu}_e}/T$, there will be *no* modifications in the capture rates. Likewise for the inverse process of positron capture on protons, $e^+ + n \to p + \bar{\nu}_e$. In this case, there will be no alteration of the final state $\bar{\nu}_e$ blocking factor unless $\bar{\epsilon} > E^{\rm thresh}_{\bar{\nu}_e}/T$.

For example, consider the case with $L_{\nu_e} \approx -0.0343$ ($\eta_{\nu_e} = -0.05$) and $L_{\nu_\mu} = L_{\nu_\tau} = -0.15$. This gives the opposite sign potential lepton number from the case first considered above, $\mathcal{L}_e \approx -0.368$. This implies that in the smooth, adiabatic resonance sweep scenario that $\bar{\epsilon} \approx 2.724$. The neutron-to-proton ratio for this $\bar{\nu}_e$ degeneracy parameter, but neglecting the effects of $\bar{\nu}_e$ conversion, is of course completely ruled out by the data:

$$\left.\frac{n}{p}\right|^{\eta_{\nu_e}=-0.05}_{\bar{\epsilon}=0} \approx 0.263. \tag{68}$$

When the conversion of $\bar{\nu}_e$'s to sterile neutrinos is taken into account, we get a result which is still unacceptable and only incrementally better,

$$\left.\frac{n}{p}\right|^{\eta_{\nu_e}=-0.05}_{\bar{\epsilon}=2.724} \approx 0.260. \tag{69}$$

The very small effect of active-sterile neutrino conversion in this case is because at Weak Freeze Out, $T \approx 0.7\,{\rm MeV}$, the scaled threshold energy is $E^{\rm thresh}_{\bar{\nu}_e}/T_{\rm wfo} \approx 2.58$, a value not much smaller than $\bar{\epsilon}$.

If we try to circumvent this threshold problem by invoking even larger negative lepton number, we are usually still left with an unacceptably high neutron-to-proton ratio. For example, consider the case with $L_{\nu_e} \approx -0.343$ ($\eta_{\nu_e} = -0.05$) and $L_{\nu_\mu} = L_{\nu_\tau} = -0.2$. This gives the opposite sign potential lepton number from the case

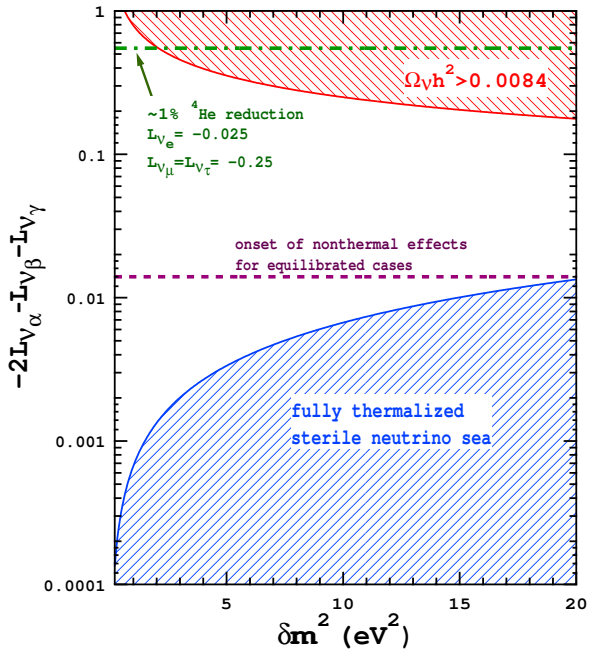

FIG. 7: Constraints and guidelines as in Fig.s (5) & (6), but now for negative values of potential lepton number. The dot-dashed line represents the vicinity of parameter space in a no active-active mixing scenario where the ^{4}He yield is reduced by about 4% over the standard value, giving agreement with the observationally-inferred helium abundance. The dashed line gives a rough threshold on potential lepton number in the equilibrated regime ($L_e = L_\mu = L_\tau$) beyond which significant alterations in ^{4}He yield stemming from $\bar{\nu}_e$ spectral distortion can be expected.

first considered above, $\mathcal{L}_e \approx -0.4685$ and $\bar{\epsilon} \approx 3.262$, a value now significantly above the scaled threshold. The neutron-to-proton ratio at Weak Freeze Out in this case would be roughly

$$\left.\frac{n}{p}\right|^{\eta_{\nu_e}=-0.05}_{\bar{\epsilon}=3.262} \approx 0.163, \qquad (70)$$

a prodigious 38% decrease over the result in Eq. (68), but still likely unacceptably large, mostly on account of the pernicious effects of the degeneracy in $\bar{\nu}_e$. Could we then consider large negative lepton numbers in the ν_μ and ν_τ neutrinos, but near zero excess of $\bar{\nu}_e$. The answer is no, because in any realistic scenario active-active conversion will keep lepton numbers in all neutrino flavors within an order of magnitude of each other [13].

In the no active-active mixing limit, initial lepton numbers $L_{\nu_e} = -0.025$ and $L_{\nu_\mu} = L_{\nu_\tau} = -0.25$ provide a distortion in the $\bar{\nu}_e$ spectrum which gives an acceptable n/p ratio corresponding to a slightly lower ^{4}He yield than in standard zero-lepton number BBN. However, this big lepton number disparity is not likely possible with efficient active-active mixing. For all cases where active neutrinos are equilibrated, a potential lepton number larger in magnitude (more negative than) -0.014 results in significant modification (bigger than a half percent or so) in the ^{4}He yield over the no-distortion BBN result. Fig. (7) summarizes these considerations. Again, the warning as to the very rough nature of our guidelines applies here as well as in Fig. (6).

V. DISCUSSION AND CONCLUSIONS

The most general conclusion that can be drawn from this work is the existence of one or more light sterile neutrinos could alter the relationship between neutrino chemical potential and primordial nucleosynthesis yields. An ancillary conclusion is that it may not always be true that invocation of a net lepton number in excess of that given in Eq. (2) can reconcile an LSND-inspired light sterile neutrino with Big Bang Nucleosynthesis limits. A lepton number with magnitude $L \geq 10^{-2}$ will certainly suppress sterile neutrino production for epochs with temperatures above that of Weak Decouplig, $T_{\rm dec} \approx 3\,{\rm MeV}$, but at the price of driving coherent active-to-sterile neutrino conversion in the regime below Weak Decoupling and, depending on $\delta m^2_{\rm as}$, potentially above Weak Freeze Out. In turn, this will lead to depleted, non-thermal ν_e or $\bar{\nu}_e$ energy distribution functions which can modify the neutron-to-proton ratio and, hence, the ^{4}He yield over the standard BBN case.

We have shown that in the $\nu_e \to \nu_s$ neutrino flavor conversion channel these modifications lead to generally larger neutron-to-proton ratios at Weak Freeze Out and therefore to a generally larger ^{4}He yield than in the standard BBN case. In some circumstances this may be unacceptable as discussed in the last section.

In contrast, invocation of non-thermal $\bar{\nu}_e$ energy spectra stemming from negative potential lepton number-driven active-sterile neutrino flavor conversion in the channel $\bar{\nu}_e \to \bar{\nu}_s$ is not nearly as vulnerable to constraint. This is because the threshold in the lepton capture reactions on free nucleons dictates that only non-thermal deficits in the $\bar{\nu}_e$ energy distribution which extend to energies beyond the threshold can affect the rates. Since the initial lepton numbers would have to be very large to to produce deficits extending beyond the threshold, it is not likely that the effects discussed here can be used to extend constraints.

Simplistic limits on sterile neutrinos based on *conventional* BBN calculations with thermal lepton energy distribution functions are now suspect. If the miniBooNE experiment sees evidence for neutrino mixing in the LSND range or beyond we will be forced to re-think the BBN paradigm, incorporating the effects pointed out here.

This would also force us to confront the problem posed by the work in this paper. Namely, what are the light element primordial nucleosynthesis abundance yields when both active-active and active-sterile neutrino inter-conversion/mixing among eight neutrino species is followed simultaneously and consistently with lepton cap-

ture/decay and nuclear reactions? This is a challenging problem at present that pushes the limits of our understanding of neutrino physics and neutrino flavor conversion in dense and hot environments.

Acknowledgments

The work of G.M.F. was supported in part by NSF grant PHY-00-99499, the TSI collaboration's DOE SciDAC grant, and a UC/LANL CARE award at UCSD; K.A. was supported by Los Alamos National Laboratory (under DOE contract W-7405-ENG-36) and also acknowledges the UC/LANL CARE award. N.B. was supported by Fermilab, which is operated by URA under DOE contract No. DE-AC02-76CH03000, and was additionally supported by NASA under NAG5-10842. This research was supported in part by the National Science Foundation under Grant No. PHY99-07949 at the KITP. The authors thank the ECT* and the INT at the University of Washington for hospitality. We thank Ray Volkas and Robert Foot for discussions.

[1] K. Eitel, New J. Phys. **2**, 1 (2000).
[2] G. McGregor [MiniBooNE Collaboration], AIP Conf. Proc. **655**, 58 (2003).
[3] H. Murayama and T. Yanagida, Phys. Lett. B **520**, 263 (2001); G. Barenboim, L. Borissov, J. Lykken and A. Y. Smirnov, JHEP **0210**, 001 (2002).
[4] M. C. Gonzalez-Garcia, M. Maltoni and T. Schwetz, Phys. Rev. D **68**, 053007 (2003).
[5] K. N. Abazajian, Astropart. Phys. **19**, 303 (2003); P. Di Bari, Phys. Rev. D **65**, 043509 (2002) [Addendum-ibid. D **67**, 127301 (2003)].
[6] R. H. Cyburt, B. D. Fields, K. A. Olive, and E. Skillman, astro-ph/0408033.
[7] K. A. Olive and E. Skillman, astro-ph/0405588.
[8] S. Hannestad, JCAP **0305**, 004 (2003); . Pierce and H. Murayama, Phys. Lett. B **581**, 218 (2004).
[9] M. Tegmark *et al.* [SDSS Collaboration], astro-ph/0310723; D. N. Spergel *et al.*, Astrophys. J. Suppl. **148**, 175 (2003).
[10] U. Seljak *et al.*, astro-ph/0407372.
[11] R. Foot and R. R. Volkas, Phys. Rev. Lett. **75**, 4350 (1995).
[12] S.P. Mikheyev and A.Yu. Smirnov, Yad. Fiz. **42**, 1441 (1985) [Sov. J. Nucl. Phys. **42**, 913 (1985)]; L. Wolfenstein, Phys. Rev. D **17**, 2369 (1978).
[13] A. D. Dolgov, S. H. Hansen, S. Pastor, S. T. Petcov, G. G. Raffelt and D. V. Semikoz, Nucl. Phys. B **632**, 363 (2002); K. N. Abazajian, J. F. Beacom and N. F. Bell, Phys. Rev. D **66**, 013008 (2002); Y. Y. Y. Wong, Phys. Rev. D **66**, 025015 (2002).
[14] V. Barger, J. P. Kneller, P. Langacker, D. Marfatia and G. Steigman, Phys. Lett. B **569**, 123 (2003);
[15] D. P. Kirilova, Astropart. Phys. **19**, 409 (2003).
[16] K. Abazajian, X. Shi and G. M. Fuller, arXiv:astro-ph/9909320.
[17] J. P. Kneller, R. J. Scherrer, G. Steigman and T. P. Walker, Phys. Rev. D **64**, 123506 (2001).
[18] X. Shi and G. M. Fuller, Phys. Rev. Lett. **82**, 2832 (1999).
[19] Y.-Z. Qian and G. M. Fuller, Phys. Rev. D **51**, 1479 (1995).
[20] A. B. Balantekin and G. M. Fuller, Phys. Lett. **B471**, 195 (2000).
[21] G. C. McLaughlin, J. M. Fetter, A. B. Balantekin and G. M. Fuller, Phys. Rev. C **59**, 2873 (1999).
[22] Y. Z. Qian, G. M. Fuller, G. J. Mathews, R. Mayle, J. R. Wilson and S. E. Woosley, Phys. Rev. Lett. **71**, 1965 (1993).
[23] J. M. O'Meara, D. Tytler, D. Kirkman, N. Suzuki, J. X. Prochaska, D. Lubin and A. M. Wolfe, Astrophys. J. **552**, 718 (2001).
[24] K. A. Olive, E. Skillman and G. Steigman, Astrophys. J. **483**, 788 (1997).
[25] Y. I. Izotov and T. X. Thuan, Astrophys. J. **602**, 200 (2004).
[26] M. Sorel, J. M. Conrad and M. Shaevitz, arXiv:hep-ph/0305255.
[27] C. Y. Cardall and G. M. Fuller, Astrophys. J. **472**, 435 (1996).
[28] G. M. Fuller, W. A. Fowler, M. J. Newman, Astrophys. J. **293**, 1 (1985).

APPENDIX A: WEAK RATES WITH NON-THERMAL NEUTRINO ENERGY SPECTRA

In this Appendix we calculate the forward and reverse rates of the processes in Eqs. (56) & (57) for the cases where, respectively, all neutrinos below energy $E_{\nu_e} = T\epsilon$ or antineutrinos below energy $E_{\overline{\nu}_e} = T\overline{\epsilon}$ are converted to sterile species. We provide estimates of these rates in terms of standard relativistic Fermi integrals. We also discuss how these rates would be modified if the MSW resonance does not sweep smoothly and continuously (and adiabatically) through the low energy neutrino or antineutrino distribution function, but instead skips to higher energies. The rate modifications for Cases 1 and 2 in the efficient active-active neutrino mixing limit will be different, of course, because in those scenarios the "holes" in the neutrino distribution functions are not empty. Though the rate formulae presented here are not valid for these cases, they still give a general idea of how the lepton capture/decay rates depend on spectral distortion and thresholds.

If there is no active-sterile conversion and all neutrino, nucleon, and charged lepton distribution functions are thermal in character, the ν_e capture rate on neutrons is $\lambda^0_{\nu_e n}$. By contrast, we will denote as $\lambda_{\nu_e n}$ the actual electron neutrino capture rate when the same thermodynamic conditions obtain, but now where ν_e's have been converted to sterile species up to scaled energy ϵ as out-

lined above. If all neutrino, nucleon, and charged lepton energy distribution functions are at least piece-wise Fermi-Dirac or zero, these rates can be written [28], respectively, as

$$\lambda^0_{\nu_e n} \approx \Lambda\left[1 - e^{\eta_e - \eta_{\nu_e} - \xi_{np}}\right]^{-1} \int_0^\infty x^2 (x + \xi_{np})^2 \left(\frac{1}{e^{x - \eta_{\nu_e}} + 1} - \frac{1}{e^{x + \xi_{np} - \eta_e} + 1}\right) dx, \tag{A1}$$

$$\begin{aligned} \lambda_{\nu_e n} &\approx \Lambda\left[1 - e^{\eta_e - \eta_{\nu_e} - \xi_{np}}\right]^{-1} \int_\epsilon^\infty x^2 (x + \xi_{np})^2 \left(\frac{1}{e^{x - \eta_{\nu_e}} + 1} - \frac{1}{e^{x + \xi_{np} - \eta_e} + 1}\right) dx \\ &\approx \Lambda\left[1 - e^{\eta_e - \eta_{\nu_e} - \xi_{np}}\right]^{-1} \sum_{n=0}^{4} \alpha_n \left[F_n\left(\eta_\nu^{\rm eff}\right) - F_n\left(\eta_e^{\rm eff}\right)\right]. \end{aligned} \tag{A2}$$

Here the integration variable in both equations is the scaled ν_e energy, $x = E_{\nu_e}/T$. The final state electron energy is $E_e = T\,(x + \xi_{np})$. The other notation in these expressions is as defined above and $\xi_{np} \equiv Q_{np}/T$ with $Q_{np} = \delta m_{np}$. There is no threshold for ν_e energy in this reaction channel. The temperature and matrix element-dependent factor in both rate expressions is

$$\begin{aligned} \Lambda &\equiv \langle G \rangle \frac{\ln 2}{\langle ft \rangle} \left(\frac{T}{m_e c^2}\right)^5 \\ &\approx \left(1.835 \times 10^{-2}\,{\rm s}^{-1}\right) \langle G \rangle \left(\frac{T}{\rm MeV}\right)^5, \end{aligned} \tag{A3}$$

where $\langle ft \rangle$ is the effective ft-value as defined in Ref. [28] and is roughly $\log_{10} ft \approx 3.035$ for free nucleons, while $\langle G \rangle$ is the average Coulomb wave correction factor (also defined in Ref. [28]) with $G \equiv F(Z, E_e) E_e/p_e$ and where $F(Z, E_e)$ is the usual Fermi function for nuclear charge Z and final state electron energy E_e. For the relativistic leptons considered here (the lowest electron energy is $\approx Q_{np} \approx 1.3\,{\rm MeV}$), $\langle G \rangle \approx 1$, though we note that $\langle G \rangle$ in the no-transformation case is slightly larger than that for the case with the ϵ cut-off on account of the lower energy electrons present in the phase space integral in the former case. (Electrons are "pulled in" to the proton because of Coulomb attraction, making for a larger overlap.)

The second approximation in Eq. (A2) gives $\lambda_{\nu_e n}$ as a sum of differences of relativistic Fermi integrals. In this expression the effective ν_e and e^- degeneracy parameters are defined as $\eta_\nu^{\rm eff} \equiv \eta_{\nu_e} - \epsilon$ and $\eta_e^{\rm eff} \equiv \eta_e - \delta$, respectively, where $\delta \equiv \epsilon + \xi_{np}$. Also in Eq. (A2) we define $\alpha_4 \equiv 1$, while $\alpha_3 \equiv 2\,(\epsilon + \delta)$, and $\alpha_2 \equiv (\epsilon + \delta)^2 + 2\epsilon\delta$, with $\alpha_1 \equiv 2\epsilon\delta\,(\epsilon + \delta)$ and $\alpha_0 \equiv \epsilon^2\delta^2$. Note that as $\epsilon \to 0$, both expressions in Eq. (A2) approach $\lambda^0_{e^- p}$ in Eq. (A1). It is obvious that for nonzero ϵ the ν_e capture rate on neutrons will be reduced over its no-transformation value, $\lambda_{\nu_e n} < \lambda^0_{\nu_e n}$.

The rate for the corresponding reverse process of electron capture on protons, $e^- + p \to n + \nu_e$, will be increased if some ν_e's are transformed to sterile states, as there will be less final state ν_e blocking in this case. For a Fermi-Dirac distribution of electrons, and in terms of an integral over electron energy E_e, this rate is

$$\lambda_{e^- p} \approx \frac{\langle G \rangle \ln 2}{\langle ft \rangle (m_e c^2)^5} \int_{Q_{np}}^\infty \frac{E_e^2\,(E_e - Q_{np})^2}{e^{E_e/T - \eta_e} + 1} \left[1 - S_{\nu_e}\right] dE_e, \tag{A4}$$

where S_{ν_e} is the energy-dependent ν_e occupation probability,

$$S_{\nu_e} = 0 \qquad \text{for } E_{\nu_e}/T \le \epsilon, \tag{A5}$$

$$S_{\nu_e} = \frac{1}{e^{E_{\nu_e}/T - \eta_{\nu_e}} + 1} \qquad \text{for } E_{\nu_e}/T > \epsilon. \tag{A6}$$

Here the ν_e energy is $E_{\nu_e} = E_e - Q_{np}$ on account of the

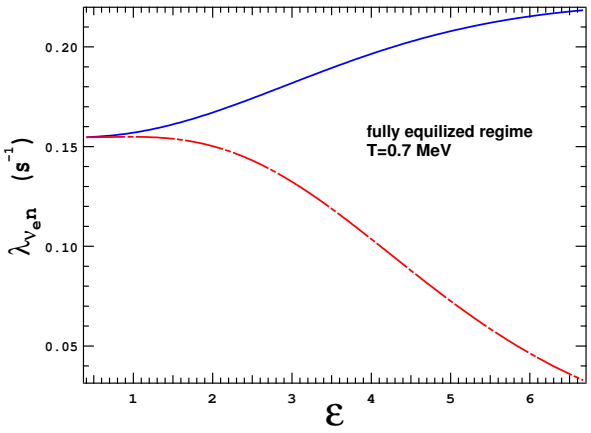

FIG. 8: Rate $\lambda_{\nu_e n}$ in ${\rm s}^{-1}$ for the process $\nu_e + n \to p + e^-$ at temperature $T = 0.7\,{\rm MeV}$ as a function of ϵ and/or L_{ν_e} in the smooth and continuous resonance sweep limit and for the case of complete active neutrino equalization ($L_{\nu_e} = L_{\nu_\mu} = L_{\nu_\tau}$). The solid curve gives the rate for no sterile neutrino conversion, thermal ν_e distribution, but with the ν_e chemical potential appropriate for the corresponding ϵ value. The dot-dashed curve gives the rate with active-sterile neutrino conversion and corresponding non-thermal character for the ν_e energy distribution function.

threshold, Q_{np}.

It is convenient to re-write the rate in Eq. (A4) as an integration over neutrino energy scaled by temperature, $x = E_{\nu_e}/T$, and as a sum of contributions from low neutrino energy with no final state blocking, and higher final state neutrino energy where there is non-zero Fermi blocking,

$$\lambda_{e^-p} = \lambda^{\rm low}_{e^-p} + \lambda^{\rm high}_{e^-p}. \tag{A7}$$

The first of these rate contributions can be approximated by

$$\lambda^{\rm low}_{e^-p} \approx \Lambda \int_0^{\epsilon} \frac{x^2\,(x+\xi_{np})^2}{e^{x+\xi_{np}-\eta_e}+1} dx. \tag{A8}$$

Just as for ν_e capture, the average Coulomb wave correction factor will be lower (closer to unity) with increasing ϵ. Again this has to do with the enhancement of the low energy electron probability density near the proton. As above, we can represent the rate contribution in Eq. (A8) in terms of standard relativistic Fermi integrals,

$$\lambda^{\rm low}_{e^-p} \approx \Lambda\big[F_4\,(\eta_e-\xi_{np}) + 2\xi_{np}F_3\,(\eta_e-\xi_{np}) + \xi^2_{np}F_2\,(\eta_e-\xi_{np})\big] - \Lambda\sum_{n=0}^{4}\beta_n F_n\,(\eta_e-\xi_{np}-\epsilon), \tag{A9}$$

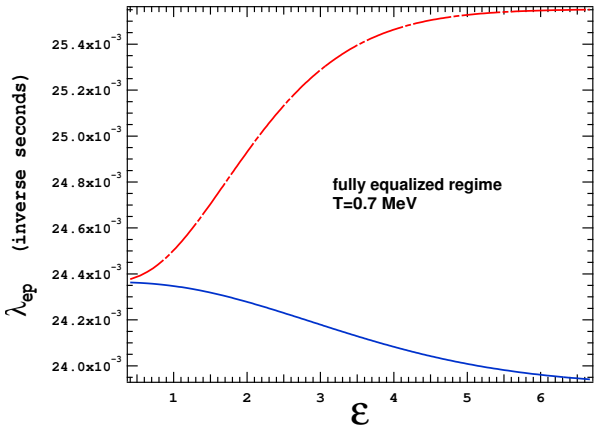

FIG. 9: Rate λ_{ep} in $\rm s^{-1}$ for the process $e^- + p \rightarrow n + \nu_e$ at temperature $T = 0.7\,\rm MeV$ as a function of ϵ and/or L_{ν_e} in the smooth and continuous resonance sweep limit and for the case of complete active neutrino equalization ($L_{\nu_e} = L_{\nu_\mu} = L_{\nu_\tau}$). The solid curve gives the rate for no sterile neutrino conversion, thermal ν_e distribution, but with the ν_e chemical potential appropriate for the corresponding ϵ value. The dot-dashed curve gives the rate with active-sterile neutrino conversion and corresponding non-thermal character of the ν_e energy distribution function.

where $\beta_4 \equiv 1$, and where $\beta_3 \equiv 2\,(\epsilon+\delta)$, while $\beta_2 \equiv (\epsilon+\delta)^2 + 2\epsilon\delta$ and $\beta_1 \equiv 2\epsilon\delta(\epsilon+\delta)$, with $\beta_0 \equiv \epsilon^2\delta^2$. Here we define $\delta \equiv \epsilon + \xi_{np}$.

The physical interpretation of this expression for $\lambda^{\rm low}_{e^-p}$ is clear if it is recalled that the ν_e energy is $E_{\nu_e} = E_e - Q_{np}$, implying that the "effective final state neutrino degeneracy parameter" is $\eta_e - \xi_{np}$ for the no-conversion case, and $\eta_e - \xi_{np} - \epsilon$ with conversion of ν_e's to steriles. Of course, as $\epsilon \rightarrow 0$, the rate contribution from the (final state ν_e) unblocked portion of the phase space approaches zero, $\lambda^{\rm low}_{e^-p} \rightarrow 0$. The second of the rate contributions in Eq. (A7) can be approximated as

$$\begin{aligned}\lambda^{\rm high}_{e^-p} &\approx \Lambda\big[1 - e^{\xi_{np}-\eta_e+\eta_{\nu_e}}\big]^{-1}\int_{\epsilon}^{\infty} x^2(x+\xi_{np})^2\left(\frac{1}{e^{x+\xi_{np}-\eta_e}+1} - \frac{1}{e^{x-\eta_{\nu_e}}+1}\right)dx \\ &\approx \Lambda\big[1 - e^{\xi_{np}-\eta_e+\eta_{\nu_e}}\big]^{-1}\sum_{n=0}^{4}\beta_n\left[F_n\,(\eta_e-\xi_{np}-\epsilon) - F_n\,(\eta_{\nu_e}-\epsilon)\right],\end{aligned} \tag{A10}$$

where the notation is as above and where the β_n are as defined above for Eq. (A9). In summary, a hole in the low

energy ν_e distribution results in a lower value for $\lambda_{\nu_e n}$, a higher value for $\lambda_{e^- p}$ and, hence, an increased n/p ratio.

By contrast, conversion up to scaled energy $\bar{\epsilon} = E_{\bar{\nu}_e}/T$ of $\bar{\nu}_e$'s to sterile neutrinos, $\bar{\nu}_e \rightarrow \bar{\nu}_s$, would result in a *lower* value of the neutron-to-proton ratio and, hence, a lower ^{4}He yield. This is because a low energy deficit in the $\bar{\nu}_e$ distribution would lead to a decreased rate for $\bar{\nu}_e + p \rightarrow n + e^+$ and, on account of less blocking, an increased rate for the reverse process. Handling the energy threshold for these reactions is, however, somewhat more complicated than for ν_e and e^- capture.

Using much the same notation as above, we can approximate the rate for $\bar{\nu}_e + p \rightarrow n + e^+$ as

$$\begin{aligned} \lambda_{\bar{\nu}_e p} &\approx \Lambda\big[1 - e^{\xi_{np} - \eta_e - \eta_{\bar{\nu}_e}}\big]^{-1} \int_{\gamma_{\rm thresh}}^{\infty} x^2 (x - \xi_{np})^2 \left(\frac{1}{e^{x - \eta_{\bar{\nu}_e}} + 1} - \frac{1}{e^{x - \xi_{np} + \eta_e} + 1} \right) dx \\ &\approx \Lambda\big[1 - e^{\xi_{np} - \eta_e - \eta_{\bar{\nu}_e}}\big]^{-1} \sum_{n=0}^{4} \bar{\alpha}_n \left[F_n\left(\eta_{\bar{\nu}}^{\rm eff}\right) - F_n\left(\eta_{\bar{e}}^{\rm eff}\right) \right]. \end{aligned} \tag{A11}$$

The integration variable in the first of these equations is $x = E_{\bar{\nu}_e}/T$, and the final state positron energy will be $E_{e^+} = T\,(x - \xi_{np})$. The scaled energy threshold in these expressions is

$$\begin{aligned} \gamma_{\rm thresh} &= \xi_{np} + m_e \quad \text{for} \quad \xi_{np} + m_e \geq \bar{\epsilon} \\ \gamma_{\rm thresh} &= \bar{\epsilon} \qquad\quad \text{for} \quad \bar{\epsilon} > \xi_{np} + m_e \end{aligned} \tag{A12}$$

where $m_e \equiv m_e c^2/T$. It is clear that transformation of $\bar{\nu}_e$'s with energies below the threshold energy $Q_{np} + m_e c^2$ does not affect the rate. In the second approximation in Eq. (A11), the effective $\bar{\nu}_e$ degeneracy parameter is $\eta_{\bar{\nu}}^{\rm eff} = \eta_{\bar{\nu}_e} - \bar{\epsilon}$, while the effective positron degeneracy parameter is $\eta_{\bar{e}}^{\rm eff} = \xi_{np} - \eta_e - \bar{\epsilon}$. (Since electromagnetic equilibrium always obtains here, the positron and electron degeneracy parameters have equal magnitudes and opposite signs, $\eta_{e^+} = -\eta_e$.) If we define $a \equiv 2\bar{\epsilon} - \xi_{np}$ and $b \equiv \bar{\epsilon}\,(\bar{\epsilon} - \xi_{np})$, then the coefficients $\bar{\alpha}_n$ are: $\bar{\alpha}_4 = 1$; $\bar{\alpha}_3 = 2a$; $\bar{\alpha}_2 = a^2 + 2b$; $\bar{\alpha}_1 = 2ab$; and $\bar{\alpha}_0 = b^2$.

Utilizing the same quantities and notation as in Eq. (A11), the rate for the reverse process of positron capture, $e^+ + n \rightarrow p + \bar{\nu}_e$, can be written as

$$\lambda_{e^+ n} \approx \frac{\Lambda}{1 - e^{\eta_e - \xi_{np} + \eta_{\bar{\nu}_e}}} \int_{\gamma_{\rm thresh}}^{\infty} x^2 (x - \xi_{np})^2 \left(\frac{1}{e^{x + \eta_e - \xi_{np}} + 1} - \frac{1}{e^{x - \eta_{\bar{\nu}_e}} + 1} \right) dx + \Lambda \int_{m_e + \xi_{np}}^{\gamma_{\rm thresh}} \frac{x^2 (x - \xi_{np})^2}{e^{x - \xi_{np} + \eta_e} + 1} dx. \tag{A13}$$

Again we see that if $\bar{\epsilon} < \xi_{np} + m_e$, then from Eq. (A12) the threshold is $\gamma_{\rm thresh} = \xi_{np} + m_e$ and the neutrino flavor conversion will have no affect on the rate. In this case, the second term of Eq. (A13) will vanish and the first term will be the rate with no neutrino conversion. The full rate expression in Eq. (A13) can be broken up into three parts,

$$\lambda_{e^+ n} = \lambda_{e^+ n}^{\rm first} + \lambda_{e^+ n}^{\rm snd} + \lambda_{e^+ n}^{\rm thrd}, \tag{A14}$$

each of which can be rendered in terms of standard relativistic Fermi integrals.

Here $\lambda_{e^+ n}^{\rm first}$ corresponds to the first integral in Eq. (A13). It can be reduced to

$$\lambda_{e^+ n}^{\rm first} \approx \frac{\Lambda}{1 - e^{\eta_e - \xi_{np} + \eta_{\bar{\nu}_e}}} \sum_{n=0}^{4} \bar{\alpha}_n \left[F_n\left(\eta_{\bar{e}}^{\rm eff}\right) - F_n\left(\eta_{\bar{\nu}}^{\rm eff}\right) \right], \tag{A15}$$

where the $\bar{\alpha}_n$ are as defined for Eq. (A11), the effective positron degeneracy parameter is $\eta_{\bar{e}}^{\rm eff} \equiv -\eta_e + \xi_{np} - \bar{\epsilon}$, and the effective $\bar{\nu}_e$ degeneracy parameter in this case is $\eta_{\bar{\nu}}^{\rm eff} \equiv \eta_{\bar{\nu}_e} - \bar{\epsilon}$.

Note that the second integral in Eq. (A13) is the sum $\lambda_{e^+ n}^{\rm snd} + \lambda_{e^+ n}^{\rm thrd}$. The last term in this sum can be approximated as

$$\lambda_{e^+ n}^{\rm thrd} \approx -\Lambda \sum_{n=0}^{4} \bar{\alpha}_n F_n\left(\xi_{np} - \eta_e - \bar{\epsilon}\right), \tag{A16}$$

where the $\bar{\alpha}_n$ are the same as defined above for Eqs. (A11) & Eq. (A15). In similar fashion we can express $\lambda_{e^+ n}^{\rm snd}$ in terms of standard relativistic Fermi integrals,

$$\lambda_{e^+ n}^{\rm snd} \approx \Lambda \sum_{n=0}^{4} \bar{\beta}_n F_n\left(-m_e - \eta_e\right). \tag{A17}$$

We define $x \equiv 2m_e + \xi_{np}$ and $y = m_e\,(m_e + \xi_{np})$, with $m_e \equiv m_e c^2/T$. With these definitions we can write the $\bar{\beta}_n$ in Eq. (A17) as: $\bar{\beta}_4 \equiv 1$, while $\bar{\beta}_3 \equiv 2x$, $\bar{\beta}_2 \equiv x^2 + 2y$, $\bar{\beta}_1 \equiv 2xy$, and $\bar{\beta}_0 \equiv y^2$.